EPA-R4-73-030a

July 1973

ENVIRONMENTAL MONITORING SERIES

URBAN AIR SHED PHOTOCHEMICAL SIMULATION MODEL STUDY

VOLUME I - DEVELOPMENT AND EVALUATION

Office of Research and Development
U.S. Environmental Protection Agency
Washington, D.C. 20460

EPA-R4-73-030a

URBAN AIR SHED PHOTOCHEMICAL SIMULATION MODEL STUDY

VOLUME I - DEVELOPMENT AND EVALUATION

by

S.D. Reynolds, Mei-Kao Lui,
T.A. Hecht, P.M. Roth, and J.H. Seinfield

Systems Applications, Inc.
9418 Wilshire Boulevard
Beverly Hills, California 90212

Contract No. 68-02-0339
Program Element No. 1A1009

EPA Project Officer: Herbert Viebrock

Meteorology Laboratory
National Environmental Research Center
Research Triangle Park, North Carolina 27711

Prepared for

OFFICE OF RESEARCH AND DEVELOPMENT
U.S. ENVIRONMENTAL PROTECTION AGENCY
WASHINGTON, D.C. 20460

July 1973

This report has been reviewed by the Environmental Protection Agency and approved for publication. Approval does not signify that the contents necessarily reflect the views and policies of the Agency, nor does mention of trade names or commercial products constitute endorsement or recommendation for use.

ABSTRACT

During the period July 1970 to June 1971, Systems Applications, Inc., under Contract CPA 70-148, undertook "Development of a Simulation Model For Estimating Ground Level Concentrations of Photochemical Pollutants". The results of this work have been presented in Roth et al. (1971), a seven volume project report which describes in detail all aspects of the year's efforts. The abstract of that report states the following:

> "In this report we describe the progress that has been achieved to date in the development and validation of a simulation model for estimating ground level concentrations of photochemical pollutants. This model is based on the finite difference solution of the equations of conservation of mass, using the method of fractional steps. The bulk of the effort reported here is developmental, involving the compilation of a comprehensive source emissions inventory, the development and validation of a kinetic mechanism for photochemical reactions, the adaptation of the method of fractional steps for use in the solution of the governing equations, and the preparation of maps displaying spatial and temporal variations in wind speed and direction and in the height of the inversion base. The details of these various efforts are described in a series of appendices to this report. Although a validated kinetic mechanism has been developed and incorporated in the simulation model, validation efforts have thus far been restricted to carbon monoxide. Provisional validation results for the Los Angeles Basin are presented."

The work that has been carried out under the present contract is a continuation of the earlier developmental study. However, while the emphasis in the initial project was on model development, we have been concerned in the present study with

- Limited model development and improvement
- Extensive evaluation of the photochemical kinetics mechanism, involving fourteen experimental studies and four hydrocarbon systems
- Extensive evaluation of the urban airshed model for the Los Angeles Basin for six days on which pollution levels were high. Five pollutants were considered -- carbon monoxide, nitric oxide, nitrogen dioxide, hydrocarbon, and ozone.

It is the purpose of this report to fully document the procedures and results of this effort.

This report consists of two parts -- Volume I, which discusses all technical aspects of the work (this document) and Volume II, which presents a description of the computer programs that embody the model and contains a user's guide.

CONTENTS

CONTENTS (Continued)

This final report includes the following Appendices:

INTRODUCTION

During the period July 1970 to June 1971, Systems Applications, Inc., under Contract CPA 70-148, undertook development of a computer-based mathematical model capable of estimating ground level concentrations of photochemical pollutants. The results of this work have been presented in Roth et al.(1971), a seven volume project report which describes in detail all aspects of the year's efforts. The work that has been carried out under the present contract is a continuation of the earlier developmental study. However, while the emphasis in the initial project was on model development, we have been concerned in the present study with

- Limited model development and improvement
- Evaluation of the photochemical kinetics mechanism, involving fourteen experimental studies and four hydrocarbon systems
- Evaluation of the urban airshed model* for carbon monoxide, nitric oxide, nitrogen dioxide, hydrocarbon, and ozone for six validation days.

It is the purpose of this report to fully document the procedures and results of this effort, which we will refer to hereafter as the Phase II study.

The report describing Phase II consists of six parts. It is broadly divided into two portions--Volume I, which discusses all technical aspects of the work (this document) and Volume II, which presents a description of the computer programs that embody the model and contains a user's guide. Volume I, however, has four technical appendices, each of which is an independent report describing a particular aspect of the work. The four appendices are:

Appendix A. Extensions and Modifications of a Contaminant Emissions Model and Inventory for Los Angeles

*We will use the term "urban airshed model" both to refer to the model developed in Phase I and validated in Phase II and to describe any model capable of simulating transport, diffusion, and reaction in the atmosphere on a regional scale.

Appendix B. Further Validation of a Generalized Mechanism Suitable for Describing Atmospheric Photochemical Reactions

Appendix C. A Microscale Model for Describing the Contribution of Local Vehicular Sources to Pollutant Concentrations Measured at Monitoring Stations

Appendix D. Numerical Integration of the Continuity Equations.

The main volume (I) itself is divided into two main parts. The first (Section II) is concerned with the urban airshed model, its theoretical foundation and its formulation, as well as with the modifications and improvements made during Phase II. The second (Section III) focuses on the validation of the model--procedures, results, and discussion and evaluation of results. Discussion of the validation of the photochemical kinetics mechanism is confined in its entirety to Appendix B; it is not considered in the main text. Moreover, with the exception of the commentary in this volume dealing with the theoretical foundations and formulation of the urban airshed model, there has been no attempt made to repeat any portion of the seven volume Phase I report by Roth et al. (1971). The interested reader is referred to this report if he wishes to obtain a full understanding of the model and its initial development.

I. AN OVERVIEW

Urban airshed models are mathematical representations of atmospheric transport and chemical reaction processes which, when combined with a source emissions inventory and pertinent meteorological data, may be used to predict pollutant concentrations as a function of time and location in the airshed. Models capable of accurate prediction over a range of meteorological and source emission conditions will serve as an important aid in urban and regional planning, including use in:

1. Simulating the effects of alternative emission control strategies on pollutant concentrations in the airshed

2. Real-time prediction in an alert warning system

3. Examining the air pollution impact of new sources, such as freeways and power plants.

A dynamic airshed simulation model that is to be generally useful in urban planning studies must meet several requirements. First, it should be capable of predicting accurately the ground level concentrations of inert pollutants, as well as those formed in the atmosphere by chemical reactions. Second, the model should have a spatial and temporal resolution appropriate for the analysis of concentration variations which occur in a city throughout the course of a day. For a typical large urban area, the horizontal spatial resolution may be of the order of a mile, and the temporal resolution, of the order of an hour. The resolution of the model will, of course, be influenced by the availability of data of similar resolution. Third, the complexity of the model, and thus the computing time and computer storage requirements, should be such that the model can be operated at a reasonable cost using computers of general availability. The objective of the combined Phase I and Phase II programs is to develop and validate an airshed simulation model for photochemical air pollution that satisfies the stated requirements.

As we have noted earlier, Phase I was primarily developmental. We first selected a suitable modeling approach, one based on the numerical integration of the nonlinear, coupled equations of conservation of mass. We then compiled a comprehensive source emissions inventory for the region to be modeled. At the same time, we undertook the development and validation of a kinetic mechanism for photochemical reactions and selected and adapted a method for numerical integration of the continuity equations. We concluded initial development with (1) preparation of

hourly maps displaying spatial and temporal variations in wind speed and direction and in the height of the inversion base for two "validation days" and (2) preparation and testing of the computer codes embodying the model. In addition, validation runs were carried out for carbon monoxide for the two days selected. We refer the reader to Roth et al. (1971) for a full discussion of the development program.

Some comments are in order at this point as to the selection of an urban area for the purpose of validation. The Los Angeles area was chosen as the region for initial application of the model for three reasons. First, the meteorological and pollutant data base in Los Angeles is one of the richest available for any major urban center. A network of nearly three dozen wind speed and direction sensors and twelve air quality monitoring stations dot the Basin. In addition, during the summer of 1969, the Scott Research Laboratories carried out an extensive data gathering program in Los Angeles (1970). Particularly valuable were the vertical temperature profile data they gathered over three sites in the Basin, thereby permitting much more accurate specification of the depth of the mixing layer than is normally possible. Second, Los Angeles smog represents the most serious and persistent incidence of photochemical air pollution in the United States. Third, because of its lack of proximity to other large urban areas, Los Angeles has an air pollution problem which is entirely locally generated. Thus, we avoid the need to account for the influx of significant amounts of pollutants from upwind areas.

In contrast to Phase I, the present, or Phase II, study has focused primarily on model evaluation To be sure, a number of modifications and improvements to the model have been made during this effort. For example, the source emissions inventory was revised and extended (particularly for automotive emissions), the numerical integration procedure was modified, a microscale model was developed for describing the contribution of local vehicular sources to pollutant concentrations measured at monitoring stations, treatment of both the chemistry and meteorology were modified, and an additional computer program was written for the purpose of data plotting and presentation. But, taken together, these efforts constitute only a relatively minor portion of the overall study. Primary attention was given to (1) evaluation of the photochemical kinetic mechanism using smog chamber data and (2) evaluation of the airshed model, first for an inert (carbon monoxide) to test the computer program and to examine the treatment of meteorological variables, then for nitric oxide (NO), nitrogen dioxide (NO_2), hydrocarbon (HC), and ozone (O_3) for six pre-selected "validation days". As we have indicated, evaluation of the kinetic mechanism is discussed fully in Appendix B. In this report, we devote our attention to evaluation of the airshed model. But first we discuss and describe the model itself.

II. THE AIRSHED MODEL

In this section we present a complete description of the model we have developed. In the first part of the section we discuss the theoretical foundation for the model, derive the governing equations, and enumerate the assumptions upon which the model is based. In the second part, we present the model as it has been developed for application purposes. In particular, we transform the governing Equation (5) into a form suitable for computation, describe the region that has been modeled, and specify the spacing and extent of the grid of nodes that has been overlaid on the region. We conclude the section by discussing the various modifications and extensions of the original formulation, as presented in Roth et al. (1971), that have been made during the current effort.

A. Theoretical Formulation of the Model

The simulation of photochemical air pollution entails giving description to the behavior of a number of chemically reactive species in the turbulent atmospheric boundary layer. Consider N chemically reactive species in a fluid. The concentration $c_i(x,y,z,t)$ of each constituent must satisfy the continuity equation,

$$\frac{\partial c_i}{\partial t} + \frac{\partial}{\partial x}(uc_i) + \frac{\partial}{\partial y}(vc_i) + \frac{\partial}{\partial z}(wc_i) = D_i\left(\frac{\partial^2 c_i}{\partial x^2} + \frac{\partial^2 c_i}{\partial y} + \frac{\partial^2 c_i}{\partial z^2}\right) + R_i(c_1,\cdots,c_N,T) + S_i(x,y,z,t) \qquad i = 1,2,\ldots,N \tag{1}$$

where u,v and w are the components of the wind velocity, D_i is the molecular diffusivity of species i in air, R_i is the rate of formation of species i by chemical reaction, T is the temperature, and S_i is the rate of emission of species i from sources. In most fluid dynamics problems involving chemical reaction, it is necessary to carry out the simultaneous solution of the coupled equations of mass, momentum and energy to account properly for the changes in c_i, u, v, w and T and the effects of the changes in each of these variables on each other. In considering air pollution, however, it is often quite reasonable to assume that the presence of pollutants in the atmosphere does not affect the meteorology to any detectable extent. An important exception is the attenuation of incoming radiation by photochemically-generated haze, a common occurrence, for example, in the Los Angeles

area during the summer and autumn months. While the variation in pollutant concentrations may, in this way, alter the energy input to the system, and thus affect both the energy and momentum equations, it is possible to incorporate this effect in the equations of continuity alone (by treating measured intensities as data) if it is not of interest to predict temperature and velocity. Thus, the equations of continuity (1) may be solved independently of the coupled Navier-Stokes and energy equations.

Since atmospheric flows are turbulent, it is customary to represent the wind velocity components as the sum of a deterministic and stochastic component; e.g., $u = \bar{u} + u'$. Substituting $u = \bar{u} + u'$, etc., into Equation (1), taking the expected value of the equation and assuming that molecular diffusion is negligible when compared with turbulent dispersion yields the following equation governing the mean concentration $\langle c_i \rangle$,*

$$\frac{\partial \langle c_i \rangle}{\partial t} + \frac{\partial}{\partial x}(\bar{u}\langle c_i \rangle) + \frac{\partial}{\partial y} + (\bar{v}\langle c_i \rangle) + \frac{\partial}{\partial z}(\bar{w}\langle c_i \rangle)$$

$$+ \frac{\partial}{\partial x}\langle u'c_i' \rangle + \frac{\partial}{\partial y}\langle v'c_i' \rangle + \frac{\partial}{\partial z}\langle w'c_i' \rangle \qquad (2)$$

$$= \langle R_i(\langle c_1 \rangle + c_1', \ldots, \langle c_N \rangle + c_N', T) \rangle + S_i(x,y,z,t)$$

where $c_i = \langle c_i \rangle + c_i'$, $\langle c_i' \rangle = 0$, and turbulent fluctuations in temperature have been neglected.

Equation (2) is the basic equation for the mean concentration of a reactive pollutant species in the atmosphere. Its direct solution is precluded by the appearance of the new dependent variables, $\langle u'c_i' \rangle$, $\langle v'c_i' \rangle$, and $\langle w'c_i' \rangle$, as well as any variables of the form $\langle c_i'c_j' \rangle$ which arise from $\langle R_i \rangle$. Considerable attention has been given to means for approximating

* We employ different notation for the mean wind components, $\bar{u}$, $\bar{v}$, and $\bar{w}$, and the mean concentrations $\langle c_i \rangle$. The bars are used for time-averaged quantities, whereas the brackets are used for ensemble-averaged quantities.

the variables $\langle u'c_i' \rangle$, $\langle v'c_i' \rangle$, and $\langle w'c_i' \rangle$ (see for example, Kraichnan (1962), Saffman (1969), and Monin and Yaglom (1971)). The simplest and most popular means is through the so-called K-theory (Calder, 1949; Pasquill, 1962; Monin and Yaglom, 1971) in which one sets

$$\langle u'c_i' \rangle = - K_{xx} \frac{\partial \langle c_i \rangle}{\partial x} \qquad \langle v'c_i' \rangle = - K_{yy} \frac{\partial \langle c_i \rangle}{\partial y} \qquad \langle w'c_i' \rangle = - K_{zz} \frac{\partial \langle c_i \rangle}{\partial z} \tag{3}$$

It is well known that in the proper general form of the K-theory, the set of quantities K_{xx}, K_{xy}, etc. constitute the components of a second order tensor $\underline{\underline{K}}$. In most reported applications of the K-theory, off-diagonal terms of the form K_{xy}, etc. are set equal to zero. For the diagonal form of $\underline{\underline{K}}$ to be valid at all points of the region it is necessary for the tensor to have the coordinate axes as principal axes at all points of space. Such a situation can occur in the surface layers of the atmosphere, where the mean wind vector can be regarded as everywhere parallel to a given vertical plane (Calder, 1965). In a large airshed this is clearly not the case. If it is possible to assume merely that the mean velocity is parallel to the ground, with components $u \neq 0$, $v \neq 0$, $w = 0$, then the only valid form of the K-theory, as given by Equation (3), can be that in which $K_{xx} = K_{yy}$. Henceforth, we denote K_{xx} and K_{yy} as K_H, and K_{zz} as K_V.

While there has been considerable study of means for relating the variables $\langle u'c_i' \rangle$, $\langle v'c_i' \rangle$, and $\langle w'c_i' \rangle$ to the mean concentrations, there has been comparatively little examination of approximations for terms of the form $\langle c_i'c_j' \rangle$ which arise when chemical reactions are taking place in turbulence.* This lack of study is primarily a result of both the enormous theoretical difficulties associated with the description of turbulent chemical reactions and the lack of experimental data against which to compare the predictions of the turbulence theories which have been developed.* As a consequence of this situation, we make one final

*We refer the reader to Corrsin (1958), Lee (1966), and O'Brien (1966, 1968ab, 1969, 1971) for further information concerning initial studies of means for approximating joint moments of the $\langle c_i'c_j' \rangle$. In spite of these studies, it is still not possible to assess the importance of the contribution of fluctuating terms of the form $\langle c_i'c_j' \rangle$ to the mean rate of reaction $\langle R_i \rangle$ in atmospheric chemical reactions, although an initial effort along these lines has been made by Donaldson and Hilst (1972).

simplifying assumption relative to Equation (2), namely that the mean rate of reaction can be approximated by the rate based on the mean concentrations; i.e.,

$$\langle R_i(\langle c_1\rangle + c_1', \ldots, \langle c_N\rangle + c_N', T)\rangle \cong R_i(\langle c_1\rangle, \ldots, \langle c_N\rangle, T) \tag{4}$$

Substituting Equations (3) and (4) into (2) yields

$$\frac{\partial\langle c_i\rangle}{\partial t} + \frac{\partial}{\partial x}(\bar{u}\langle c_i\rangle) + \frac{\partial}{\partial y}(\bar{v}\langle c_i\rangle) + \frac{\partial}{\partial z}(\bar{w}\langle c_i\rangle)$$

$$= \frac{\partial}{\partial x}\left(K_H \frac{\partial\langle c_i\rangle}{\partial x}\right) + \frac{\partial}{\partial y}\left(K_H \frac{\partial\langle c_i\rangle}{\partial y}\right) + \frac{\partial}{\partial z}\left(K_V \frac{\partial\langle c_i\rangle}{\partial z}\right) \tag{5}$$

$$+ R_i(\langle c_1\rangle, \ldots, \langle c_N\rangle, T) + S_i(x,y,z,t)$$

Contrary to the impression conveyed in a number of earlier air pollution modeling studies, Equation (5) is *not* the fundamental equation governing the dynamic behavior of air pollutants in the atmosphere; rather, by virtue of Equations (3) and (4), it is an approximate equation, valid only under certain circumstances. We shall employ Equation (5) as the basic model in this study. However, before doing so, it is necessary to consider the limitations inherent in Equation (5) that restrict its applicability in describing the transport and reactions of air pollutants in the atmosphere.

Assessing the validity of Equation (5) for modeling air pollutant dynamics has been the subject of two recent studies (Lamb, 1973; Lamb and Seinfeld, 1973). It has been shown in these studies that Equation (5) is a valid representation of atmospheric transport and chemical reaction provided that the:

1. Time resolution of the model, Δt , is large compared with the Lagrangian time scale of the turbulence.

2. Characteristic temporal and spatial scales for gradients in the mean velocity field are large compared with the time resolution Δt and the average distance that a fluid particle travels in Δt.

3. Characteristic temporal and spatial scales for gradients in the turbulent velocity correlations are large compared with the time resolution Δt and the average distance that a fluid particle travels in Δt.

4. Characteristic temporal and spatial scales for gradients in the source emission functions S_i are large compared with Δt and the distance a particle travels in Δt.

5. Characteristic temporal scale for changes in the rate of generation or depletion of species by chemical reaction, R_i, is large compared with Δt.

These conditions may be expressed more precisely in quantitative forms. In particular, conditions 2 and 3 imply that each of the fluid velocity components should satisfy the requirements*:

$$\frac{1}{\bar{u}_i}\frac{\partial \bar{u}_i}{\partial t} \ll \frac{1}{\Delta t} \qquad i = 1,2,3$$

$$\frac{1}{\bar{u}_i}\frac{\partial \bar{u}_i}{\partial x_k} \ll [(R_{kk} + \bar{u}^2{}_k \Delta t)\Delta t]^{-1/2}$$

$$\frac{1}{\langle u_i' u_j' \rangle}\frac{\partial \langle u_i' u_j' \rangle}{\partial t} \ll \frac{1}{\Delta t} \qquad i,j = 1,2,3$$

$$\frac{1}{\langle u_i' u_j' \rangle}\frac{\partial \langle u_i' u_j' \rangle}{\partial x_k} \ll [(R_{kk} + \bar{u}_k^2 \Delta t)\Delta t]^{-1/2}$$

*For convenience in stating these conditions we employ the notation u_1, u_2, u_3 and x_1, x_2, x_3 in place of u,v,w and x,y,z, respectively.

where $R_{kk}(\underline{x},t)$ is the Lagrangian time correlation function,

$$R_{kk}(\underline{x},t) = \int_0^\infty \langle v_k(\underline{x},t)\, v_k(\underline{x},t+\tau)\rangle \, d\tau \qquad k = 1,2,3$$

and $v_k(\underline{x},t)$ is the Lagrangian velocity at position $\underline{x}$ and time t. Conditions 4 and 5 can be written as:

$$\frac{1}{S_i}\frac{\partial S_i}{\partial t} << \frac{1}{\partial t} \qquad i = 1,2,\ldots,N$$

$$\frac{1}{S_i}\frac{\partial S_i}{\partial x_k} << [R_{kk} + \bar{u}_k^2 \Delta t)\ \Delta t]^{-\frac{1}{2}} \qquad k = 1,2,3$$

$$\frac{1}{R_i}\frac{\partial R_i}{\partial t} << \frac{1}{\Delta t} \qquad i = 1,2,\ldots,N$$

These conditions, of course, impose restrictions on t and on the temporal and spatial resolution of the velocity field and the source emission functions that are to be used in Equation (5). Therefore, we must determine the extent to which these restrictions apply for conditions typically observed in the Los Angeles Basin. Only then can we specify the appropriate spatial and temporal scales for the model.

In the Los Angeles airshed there are roughly three dozen wind monitoring stations, with an average separation between them of roughly seven miles. At most stations the wind speed and direction data are averaged over a one-hour period. From these hourly-average values the mean surface wind field, $\bar{u}(x,y,t)$ and $\bar{v}(x,y,t)$, can be constructed. Subtracting the mean values from the instantaneous readings at each

station and averaging over time yields the Eulerian correlations $\langle u_i' u_j' \rangle$, i,j = 1,2,3. An Eulerian time scale for the turbulence,

$$\tau_E = \max_{i,j,\underline{x},t} \left\{ \frac{1}{\langle u_i'(\underline{x},t) u_j'(\underline{x},t) \rangle} \int_0^\infty \langle u_i'(\underline{x},t) u_j'(\underline{x},t+\tau) \rangle \, d\tau \right\}$$

can be estimated from these correlations. Although the precise relationship between the Eulerian and Lagrangian time scales, τ_E and τ_L, where

$$\tau_L = \max_{i,j,\underline{x},t} \left\{ \frac{1}{\langle u_i'(\underline{x},t) u_j'(\underline{x},t) \rangle} \int_0^\infty \langle v_i(\underline{x},t) v_j(\underline{x},t+\tau) \rangle \, d\tau \right\} ,$$

is unknown, a convenient estimate is that $\tau_L \simeq 4\tau_E$ (Hay and Pasquill, 1959). Having estimated τ_L from the wind station data, for the condition that $\Delta t >> \tau_L$, we can place a lower limit on Δt, such as $5\tau_L$. Using a $\Delta t >> \tau_L$ insures that the four conditions pertaining to the fluid velocity components will be satisfied.

Once Δt has been selected, we must specify the spatial and temporal resolutions for S_i and the temporal resolution for R_i that satisfy the final three conditions. These conditions will determine the degree of detail required for the source emissions inventory and the chemical reaction mechanism, one which is commensurate with that of the meteorological data.

Unfortunately, data of the type needed to estimate the Eulerian time scale of the turbulence in the Los Angeles Basin are not generally available. In an effort to gather data of this type, Lamb and Neiburger (1970) measured the turbulent structure of the atmosphere at a height of 20 meters in West Los Angeles. The wind velocities were averaged over a period of T = 0.3 hours. From these data, τ_E was estimated to be 50 seconds. Assuming that $\tau_L \simeq 4\tau_E$, τ_L equals 200 seconds. We therefore estimate that $\Delta t \geq 10^3$ seconds on the basis that $\Delta t \geq 5\tau_L$. The Lagrangian correlation functions were estimated to be: $R_{11} \simeq 100$ $m^2 sec^{-1}$,

$R_{22} \simeq 100\ m^2 sec^{-1}$, and $R_{33} \simeq 10\ m^2 sec^{-1}$. With $\Delta t = 10^3$ seconds and these values of the R_{kk}, the conditions limiting the validity of Equation (5) assume the quantitative values shown in Table 1. Since the conditions in Table 1 are based on data for which the averaging time was 0.3 hours, they are less stringent than those based on data for which the averaging time is 1 hour.

We have found that the minimum temporal and horizontal spatial resolution in the source emission function must be 10^3 seconds and 2000 meters, respectively. Thus, the averaging time and distance for source emissions should be, say, at least twice these values. We note that, in spite of the fact that many major pollutant sources are point and line sources, emissions must be averaged over relatively large distances to conform with the resolution of Equation (5). In the source emissions inventory described in Appendices A of Roth et al. (1971) and this report, we have spatially and temporally averaged source emissions over 2 miles (approximately 3000 meters) and 1 hour, respectively Thus, the spatial averaging we have employed is of somewhat finer resolution than that suggested by the conditions in Table 1. The condition on R_i states that the characteristic time scale for changes in the concentrations as a result of chemical reaction should be greater than 10^3 seconds--perhaps of the order of one hour. Finally, Lamb and Neiburger (1970) estimated that the minimum vertical resolution of concentration changes is of the order of 20 meters or greater. The minimum vertical mesh spacing employed is roughly 20 meters.

In summary, we find that Equation (5) is applicable in resolving those perturbations in the concentration field which have horizontal scales greater than 2 kilometers, vertical scales greater than 20 meters, and temporal scales greater than 10^3 seconds. These conditions serve as a guide to the choice of grid size and averaging time to be used in the solution of Equation (5).

*In the early morning, in order to account for the nonuniform distribution of trip starts, motor vehicle emissions are temporally averaged over 15-minute periods for the first hour (6-7 a.m.).

Table 1. Conditions Limiting Equation (5) Based on the Measurements of Wind Turbulence of Lamb and Neiburger (1970).

1. Source emission function	$\frac{1}{S_i}\frac{\partial S_i}{\partial t}$	$\ll 10^{-3}\,\text{sec}^{-1}$
	$\frac{1}{S_i}\frac{\partial S_i}{\partial x_k}$	$\ll \frac{1}{2000}\,\text{meter}^{-1}$, k = 1,2
2. Chemical reaction rate	$\frac{1}{R_i}\frac{\partial R_i}{\partial t}$	$\ll 10^{-3}\,\text{sec}^{-1}$
3. Mean velocity components	$\frac{1}{\bar{u}_i}\frac{\partial \bar{u}_i}{\partial t}$	$\ll 10^{-3}\,\text{sec}^{-1}$
	$\frac{1}{\bar{u}_i}\frac{\partial \bar{u}_i}{\partial x_k}$	$\ll \frac{1}{2000}\,\text{meter}^{-1}$, k = 1,2
		$\ll \frac{1}{20}\,\text{meter}^{-1}$, k = 3
4. Turbulent velocity components	$\frac{1}{\langle u_i' u_j' \rangle}\frac{\partial \langle u_i' u_j' \rangle}{\partial t}$	$\ll 10^{-3}\,\text{sec}^{-1}$
	$\frac{1}{\langle u_i' u_j' \rangle}\frac{\partial \langle u_i' u_j' \rangle}{\partial x_k}$	$\ll \frac{1}{2000}\,\text{meter}^{-1}$, k = 1,2
		$\ll \frac{1}{20}\,\text{meter}^{-1}$, k = 3

B. The Model Developed in this Study

The model developed is based on the solution of the N coupled partial differential equations (5) defined on the region, $x_W \leq x \leq x_E$, $y_S \leq y \leq y_N$, and $h(x,y) \leq z \leq H(x,y,t)$ for $t \geq t_o$, where x_W, x_E, y_N are the west, east, south and north boundaries of the airshed, $h(x,y)$ is ground elevation above sea level at (x,y), and $H(x,y,t)$ is the elevation above sea level of the base of a temperature inversion or an assumed upper limit for vertical mixing or transport. The initial condition on Equations (5) is that the mean concentration be specified at all locations,

$$c_i(x,y,z,t_o) = f_i(x,y,z) \tag{6}$$

(At this point and henceforth, for convenience, we omit brackets on the concentrations and overbars on the velocities. However, all concentrations and velocities continue to be mean and time-averaged quantities, respectively.)

The vertical boundary conditions are:

1. $z = h(x,y)$ $\qquad - \underline{\underline{K}}\,\underline{\nabla} c_i \cdot \underline{n}_h = Q_i(x,y,t)$ (7)

where $\underline{\underline{K}}$ is the eddy diffusivity tensor,

$$\underline{\underline{K}} = \begin{bmatrix} K_H & 0 & 0 \\ 0 & K_H & 0 \\ 0 & 0 & K_V \end{bmatrix}$$

$\underline{n}_h$ is the unit vector normal to the terrain directed into the atmosphere, and Q_i is the mass flux of species i at the surface.

2. $z = H(x,y,t)$

$$\begin{aligned} &[\underline{V} c_i - \underline{\underline{K}}\,\underline{\nabla} c_i] \cdot \underline{n}_H = [\underline{V} g_i(x,y,z,t)] \cdot \underline{n}_H \qquad \text{if } \underline{V} \cdot \underline{n}_H \leq 0 \\ &- \underline{\underline{K}}\,\underline{\nabla} c_i \cdot \underline{n}_H = 0 \qquad\qquad\qquad\qquad\qquad\quad \text{if } \underline{V} \cdot \underline{n}_H > 0 \end{aligned} \tag{8}$$

where $\underline{V}$ is the advective velocity of pollutants relative to the moving inversion base, given by

$$\underline{V} = u\underline{i} + v\underline{j} + \left(w - \frac{\partial H}{\partial t}\right)\underline{k}$$

$\underline{n}_H$ is the outwardly directed unit vector normal to the surface defined by the inversion base, and g_i is the mean concentration of species i aloft (just above the inversion base).

The condition $\underline{V}\cdot\underline{n}_H \leq 0$ in equation (8) applies when material is transported into the modeling region from above the inversion base. This boundary condition simply states that the normal component of the mass flux is continuous across the upper boundary. The condition $\underline{V}\cdot\underline{n}_H > 0$ applies when pollutants are transported up through the inversion base. Because of the abrupt stability change associated with an inversion layer, it is reasonable to assume that the turbulent diffusive flux across the boundary is zero, thereby attributing any pollutant transport into the inversion layer to advection alone. The second boundary condition in Equation (8) expresses the negligibility of the turbulent diffusive flux at the inversion base.

The horizontal boundary conditions are:

$$\begin{aligned} (\underline{U}c_i - \underline{\underline{K}}\nabla c_i)\cdot\underline{n} &= \underline{U}g_i(x,y,z,t)\cdot\underline{n} && \text{if } \underline{U}\cdot\underline{n} \leq 0 \\ -\underline{\underline{K}}\nabla c_i\cdot\underline{n} &= 0 && \text{if } \underline{U}\cdot\underline{n} > 0 \end{aligned} \qquad (9)$$

where $\underline{U} = u\underline{i} + v\underline{j}$, $\underline{n}$ is the outwardly directed unit vector normal to the horizontal boundary, and g_i is the mean concentration of species i just outside the airshed boundary. The first condition is, as before, a statement of the continuity of mass flux across the boundary when the flow is directed into the airshed. The second condition specifies that the diffusive component of the total mass flux be set equal to zero when the wind is directed out of the airshed. This condition is equivalent to that conventionally employed at the exit of tubular chemical reactors (Wehner and Wilhelm, 1956), although the

conditions prevailing at the boundary of the region are not precisely the same as those at the exit of such a reactor. Since the horizontal advective component of the mass flux generally dominates the horizontal diffusive component, the error incurred due to this approximation is generally small.

In this study, we applied Equations (5) - (9) to the prediction of pollutant concentrations over much of a fifty-mile square area that includes virtually all centers of population in the Los Angeles Basin. The region was divided into a grid of 625 2-mile x 2-mile squares, 198 of which lie over oceans or mountainous terrain having no pollutant sources. These "source-free" grid squares were not included in the region actually modeled, which is shown in Figure 1. Source emissions and meteorological variables are distributed in conformance with this grid; i.e., two miles is the resolution of the model, or the spatial dimension over which all quantities are averaged. Furthermore, for reasons to be discussed, the grid actually used in the solution of Equations (5) is a three-dimensional array of five layers of cells occupying the space between the ground and the base of the inversion and lying directly over the area shown in Figure 1. Thus, each cell has a base two miles square and a height of $(H - h)/5$. The center of each cell, or node, is the point to which values of all variables are assigned or referenced. Unfortunately, due to variations in both H and h with x and y and, in the case of H, with t, the three-dimensional modeling region has an irregular "roof" and "floor". To eliminate these irregularities, which hamper the solution of the equations, we performed the following change of variables:

$$\tau = t \qquad \xi = x \qquad \eta = y \qquad \rho = \frac{z - h(x,y)}{H(x,y,t) - h(x,y)}$$

With these changes, Equations (5) becomes

$$\frac{\partial}{\partial\tau}(\Delta H c_i) + \frac{\partial}{\partial\xi}(u\Delta H c_i) + \frac{\partial}{\partial\eta}(v\Delta H c_i) + \frac{\partial}{\partial\rho}(W c_i)$$

$$= \frac{\partial}{\partial\xi}\left\{K_H \Delta H \frac{\partial c_i}{\partial\xi} - K_H\left(\frac{\partial H}{\partial\xi} + \rho\frac{\partial\Delta H}{\partial\xi}\right)\frac{\partial c_i}{\partial\rho}\right\}$$

$$+ \frac{\partial}{\partial\eta}\left\{K_H \Delta H \frac{\partial c_i}{\partial\eta} - K_H\left(\frac{\partial h}{\partial\eta} + \rho\frac{\partial\Delta H}{\partial\eta}\right)\frac{\partial c_i}{\partial\rho}\right\}$$

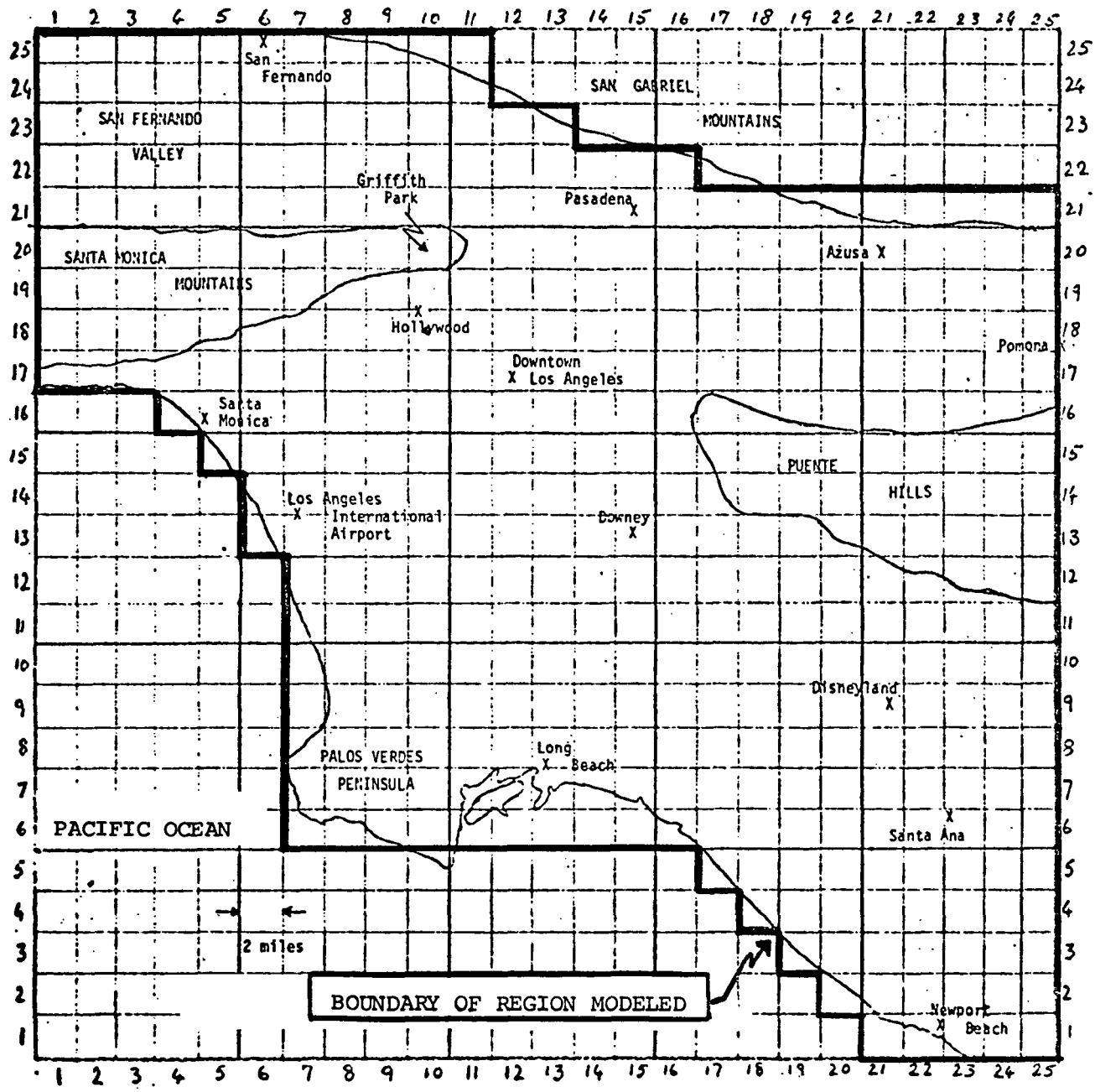

Figure 1. The Modeling Region

$$+ \frac{\partial}{\partial \rho} \left\{ - K_H \left(\frac{\partial H}{\partial \xi} + \rho \frac{\partial \Delta H}{\partial \xi} \right) \frac{\partial c_i}{\partial \xi} - K_H \left(\frac{\partial h}{\partial \eta} + \rho \frac{\partial \Delta H}{\partial \eta} \right) \frac{\partial c_i}{\partial \eta} \right.$$

$$\left. + \left(\frac{K_H}{\Delta H} \left(\frac{\partial h}{\partial \xi} + \rho \frac{\partial \Delta H}{\partial \xi} \right)^2 + \frac{K_H}{\Delta H} \left(\frac{\partial h}{\partial \eta} + \rho \frac{\partial \Delta H}{\partial \eta} \right)^2 + \frac{K_V}{\Delta H} \right) \frac{\partial c_i}{\partial \rho} \right\}$$

$$+ R_i \Delta H + S_i \Delta H \tag{10}$$

where

$$\Delta H = H(x,y,t) - h(x,y)$$

and

$$W = w - u \left(\frac{\partial h}{\partial \xi} + \rho \frac{\partial \Delta H}{\partial \xi} \right) - v \left(\frac{\partial h}{\partial \eta} + \rho \frac{\partial \Delta H}{\partial \eta} \right) - \rho \frac{\partial \Delta H}{\partial \tau}$$

The initial boundary conditions now become:

$$c_i(\xi,\eta,\rho, \tau_o) = f_i \ (\xi,\eta,\rho) \tag{11}$$

1. $\rho = 0$

$$Q_i(\xi,\eta,\tau) = - \left(\frac{K_H}{\Delta H} \left(\frac{\partial h}{\partial \xi} \right)^2 + \frac{K_H}{\Delta H} \left(\frac{\partial h}{\partial \eta} \right)^2 + \frac{K_V}{\Delta H} \right) \frac{\partial c_i}{\partial \rho}$$

$$+ K_H \left(\frac{\partial h}{\partial \xi} \right) \frac{\partial c_i}{\partial \xi} + K_H \left(\frac{\partial h}{\partial \eta} \right) \frac{\partial c_i}{\partial \eta} \tag{12}$$

2. $\rho = 1$

$$Wg_i(\xi,\eta,1,\tau) = Wc_i + K_H\left(\frac{\partial H}{\partial \xi}\right)\frac{\partial c_i}{\partial \xi} + K_H\left(\frac{\partial H}{\partial \eta}\right)\frac{\partial c_i}{\partial \eta}$$

$$-\left(\frac{K_H}{\Delta H}\left(\frac{\partial H}{\partial \xi}\right)^2 + \frac{K_H}{\Delta H}\left(\frac{\partial H}{\partial \eta}\right)^2 + \frac{K_V}{\Delta H}\right)\frac{\partial c_i}{\partial \rho}$$

if $W \leq 0$

$$0 = K_H\left(\frac{\partial H}{\partial \xi}\right)\frac{\partial c_i}{\partial \xi} + K_H\left(\frac{\partial H}{\partial \eta}\right)\frac{\partial c_i}{\partial \eta} - \left(\frac{K_H}{\Delta H}\left(\frac{\partial H}{\partial \xi}\right)^2 + \frac{K_H}{\Delta H}\left(\frac{\partial H}{\partial \eta}\right)^2 + \frac{K_V}{\Delta H}\right)\frac{\partial c_i}{\partial \rho} \quad (13)$$

if $W > 0$

3. $\xi = \xi_W$ or ξ_E

$$ug_i = uc_i - K_H\left(\frac{\partial c_i}{\partial \xi} - \frac{1}{\Delta H}\left(\frac{\partial h}{\partial \xi} + \rho\frac{\partial \Delta H}{\partial \xi}\right)\frac{\partial c_i}{\partial \rho}\right)$$

if $\underline{U}\cdot\underline{n} \leq 0$

$$0 = - K_H\left(\frac{\partial c_i}{\partial \xi} - \frac{1}{\Delta H}\left(\frac{\partial h}{\partial \xi} + \rho\frac{\partial \Delta H}{\partial \xi}\right)\frac{\partial c_i}{\partial \rho}\right) \quad (14)$$

if $\underline{U}\cdot\underline{n} > 0$

4. $\eta = \eta_S$ or η_N

$$vg_i = vc_i - K_H\left(\frac{\partial c_i}{\partial \eta} - \frac{1}{\Delta H}\left(\frac{\partial h}{\partial \eta} + \rho\frac{\partial \Delta H}{\partial \eta}\right)\frac{\partial c_i}{\partial \rho}\right)$$

$$\text{if } \underline{U}\cdot\underline{n} \leq 0$$

$$0 = -K_H\left(\frac{\partial c_i}{\partial \eta} - \frac{1}{\Delta H}\left(\frac{\partial h}{\partial \eta} + \rho\frac{\partial \Delta H}{\partial \eta}\right)\frac{\partial c_i}{\partial \rho}\right) \qquad (15)$$

$$\text{if } \underline{U}\cdot\underline{n} > 0$$

Equations (10) - (15) are the transformed form of Equations (5) - (9). Fortunately, several of the terms appearing in the above equations are small when compared with other terms and can thus be neglected. For example, in the Los Angeles Basin the changes in ground elevation and inversion height with location are generally sufficiently gradual that the derivatives, $\partial h/\partial \xi$, $\partial h/\partial \eta$, $\partial \Delta H/\partial \xi$, and $\partial \Delta H/\partial \eta$ are considerably smaller than one. With the assumption that terms in Equation (10) containing these derivatives can be neglected, this equation becomes

$$\frac{\partial}{\partial \tau}(\Delta H c_i) + \frac{\partial}{\partial \xi}(u\Delta H c_i) + \frac{\partial}{\partial \eta}(v\Delta H c_i) + \frac{\partial}{\partial \rho}(W c_i)$$

$$= \frac{\partial}{\partial \xi}\left(K_H \Delta H \frac{\partial c_i}{\partial \xi}\right) + \frac{\partial}{\partial \eta}\left(K_H \Delta H \frac{\partial c_i}{\partial \eta}\right) + \frac{\partial}{\partial \rho}\left(\frac{K_V}{\Delta H}\frac{\partial c_i}{\partial \rho}\right) \qquad (16)$$

$$+ R_i \Delta H + S_i \Delta H$$

We might note that, whereas the assumption that the derivatives $\partial h/\partial \xi$, etc. are small is generally satisfied in the flat portions of the Los Angeles airshed, it is violated in the mountainous areas, such as the Palos Verdes Hills and the Santa Monica Mountains. However, since the terms omitted in Equation (10) involve horizontal diffusion, which is generally less important than horizontal advection, we do not expect to incur significant errors in using Equation (16) even in these regions.

Under the assumptions invoked in obtaining Equation (16), the boundary conditions in Equations (12) - (15) become:

1. $\rho = 0$

$$Q_i(\xi,\eta,\tau) = -\frac{K_V}{\Delta H}\frac{\partial c_i}{\partial \rho} \tag{17}$$

2. $\rho = 1$

$$\begin{aligned} Wc_i - \frac{K_V}{\Delta H}\frac{\partial c_i}{\partial \rho} &= Wg_i(\xi,\eta,1,\tau) && \text{if } W \leq 0 \\ -\frac{K_V}{\Delta H}\frac{\partial c_i}{\partial \rho} &= 0 && \text{if } W > 0 \end{aligned} \tag{18}$$

3. $\xi = \xi_W$ or ξ_E

$$\begin{aligned} uc_i - K_H\frac{\partial c_i}{\partial \xi} &= ug_i && \text{if } \underline{U}\cdot\underline{n} \leq 0 \\ -K_H\frac{\partial c_i}{\partial \xi} &= 0 && \text{if } \underline{U}\cdot\underline{n} > 0 \end{aligned} \tag{19}$$

4. $\eta = \eta_S$ or η_N

$$\begin{aligned} vc_i - K_H\frac{\partial c_i}{\partial \eta} &= vg_i && \text{if } \underline{U}\cdot\underline{n} \leq 0 \\ -K_H\frac{\partial c_i}{\partial \eta} &= 0 && \text{if } \underline{U}\cdot\underline{n} > 0 \end{aligned} \tag{20}$$

The entire airshed is thus transformed into a three-dimensional array of cells in the (ξ,η,ρ) space having all sides parallel to a Cartesian coordinate system. The actual model, then, is based on the solution of Equations (16) - (20) and (11) over a region comprised of 427 x 5 cells.

Having specified the governing equations and having described the modeling region, we now consider those components of the model that must be developed prior to its evaluation and/or application. In particular, the following tasks must be carried out:

1. The development of a contaminant emissions inventory for the Los Angeles Basin, that is, specification of the functions $S_i(\xi,\eta,\rho,\tau)$ (elevated sources) and $Q_i(\xi,\eta,\tau)$ (ground-level sources). Refer to Appendix A of this report and Appendix A of Roth et al. (1971) for complete details.

2. The development of a kinetic mechanism capable of describing the rates of chemical reactions occurring in the atmosphere, and the adaptation of this mechanism for inclusion in the airshed model, that is, specification of the functional form of the $R_i(c_1,\ldots, c_N)$. Refer to Appendix B of this report and Appendix B of Roth et al. (1971) for complete details.

3. The development of a means for including in the model the meteorological parameters, $u(\xi,\eta,\rho,\tau)$, $v(\xi,\eta,\rho,\tau)$, $w(\xi,\eta,\rho,\tau)$, $H(\xi,\eta,\tau)$, $K_H(\xi,\eta,\rho,\tau)$ and $K_V(\xi,\eta,\rho,\tau)$. Refer to Part C of this section and Appendix C of Roth et al (1971) for complete details.

4. The selection and adaptation of a numerical method suitable for the solution of Equations (16) - (20). Refer to Appendix D of this report and Appendix D of Roth et al. (1971) for complete details.

Thus, the Appendices to both this and the Phase I report, taken together, provide a full description of all individual components of the model. In the last part of this section, we briefly enumerate, for the benefit of those who are familiar with the work completed in Phase I, the modifications and extensions to the model that have been carried out during the present effort.

C. Modifications and Extensions to Original Formulation of Model

We have divided into eight categories the discussion of modifications and extensions to the original formulation of the model that have been carried out during this study--emissions, photochemistry, meteorology, numerical analysis, the model itself, treatment of subgrid scale phenomena, the computer programs, and the interpretation of air quality data for the purposes of validation. Where a particular model change is discussed in an Appendix, we merely cite the change and make proper reference. However, a more complete discussion is given for those changes not described elsewhere in the text.

1. Emissions

a. *General.* Assignment of fractional splits of NO and NO_2 emissions from various source categories (as percent NO_2). Clarification of ambiguity in Appendix A of Roth et al (1971) concerning treatment of NO_x emissions from all sources. All NO_x emissions rates are reported as being 100% NO_2, whereas they are more nearly 100% NO. Thus, all NO_x emissions rates in the earlier report should be reduced by a factor of 30/46.

b. *Automobiles.* Adoption of average pollutant emissions rates (grams/mile) based on the Federal Driving Cycle, inclusion of a correlation between emissions rate and average speed to account for temporal and spatial variations in emissions from freeways, and incorporation of a factor to account for variations in emissions resulting from a nonuniform temporal distribution of vehicle starts. Treatment of emissions in the downtown Los Angeles area also modified.

c. *Aircraft.* Emissions from airborne operations now neglected due to their small influence on the calculated pollutant concentrations. New information included, pertaining to emissions from reciprocating aircraft engines and to average number of jet aircraft flights per day made at Los Angeles International Airport.

d. *Refineries and Distributed Fixed Sources.* Revised treatment of hydrocarbon emissions with regard to reactive/unreactive split. Incorporated assumptions as to molecular weights of emitted hydrocarbons.

All extensions and modifications cited are described in detail in Appendix A of this report.

2. Photochemistry

   a. *Addition of second hydrocarbon and NO_2-particle reaction to mechanism for validation using smog chamber data.* However, changes not included in airshed model.

   b. *Additional validation of mechanism using fourteen sets of experimental data and four hydrocarbon systems.*

   c. *Estimation of reaction rate constants for which literature values are not available.* Estimation of stoichiometric coefficients. Elimination of variable stoichiometric coefficient.

   d. *Method for estimating hydrocarbon rate constants in the atmosphere for the different validation days.* This procedure, which is discussed in more detail in Section III, involves the use of gas chromatographic data to compute average percentage (over a day) of reactive paraffins, aromatics, ethylene, and other olefins present in the atmosphere. Hydrocarbon rate constants (with O, OH, and O_3) were calculated as weighted averages of average rate constants for each group, weighted in proportion to the mole fraction of the group present in the atmosphere at the time in question. Average constants were then calculated for the entire day, as the averages at any time vary only slightly with time.

A full discussion of the photochemical mechanism and its evaluation (but not topic d above) is given in Appendix B.

3. Meteorology

There is no appendix associated with this report dealing with the treatment of meteorological variables, as there was in the Phase I report. As a result we discuss extensions and modifications in the treatment of these variables more fully than we do in the case of most other parameters.

   a. *Treatment of wind field aloft.* In Appendix C of Roth et al. (1971), pages C-39 to C-42, we outlined two procedures for estimating the speed and direction of winds aloft in the absence of a data base. Comparative tests of the two

methods, carried out during Phase II, showed little difference in predicted concentrations. Due to this observation and the fact that the first method requires far less computation, we adopted the first method as the standard procedure for estimating wind speed and direction in all layers of cells above the ground. The method is based on the assumption that

$$\frac{\partial u}{\partial x} + \frac{\partial v}{\partial y} + \frac{\partial \omega}{\partial z} = 0 \quad \text{and} \quad \frac{\partial u}{\partial z} = \frac{\partial v}{\partial y} = 0$$

b. *Treatment of surface wind fields.* In Appendix C, Section II, of Roth et al. (1971) we describe the procedures used in the construction of hourly surface wind maps. These maps, which are illustrated in Figures C-17 to C-19 of that report, are detailed representations of the flow fields, representations that several of us believed could not be justified, given the level of consistency and accuracy of the available meteorological data. We felt that the wind maps should be no more complex than the data could support and thus elected to prepare less detailed maps. The newly drawn maps, illustrated in Figures 2,3, and 4 for the same three times on 29 September 1969 as the maps in Figures C-17 to C-19, are much smoother and simpler; yet they appear to provide "good representation" of the data.

Using the revised maps, we carried out validation experiments for carbon monoxide to compare predictions with those calculated using the original wind maps. Estimated concentrations based on use of the revised maps showed significant improvements when compared with air quality data reported by those monitoring stations for which discrepancies between original predictions and measured values were large. In only a few cases did discrepancies between prediction and measurement increase when the revised maps were used. Based on these observations we concluded that the initially prepared maps are more elaborate and detailed than is either necessary or justifiable.

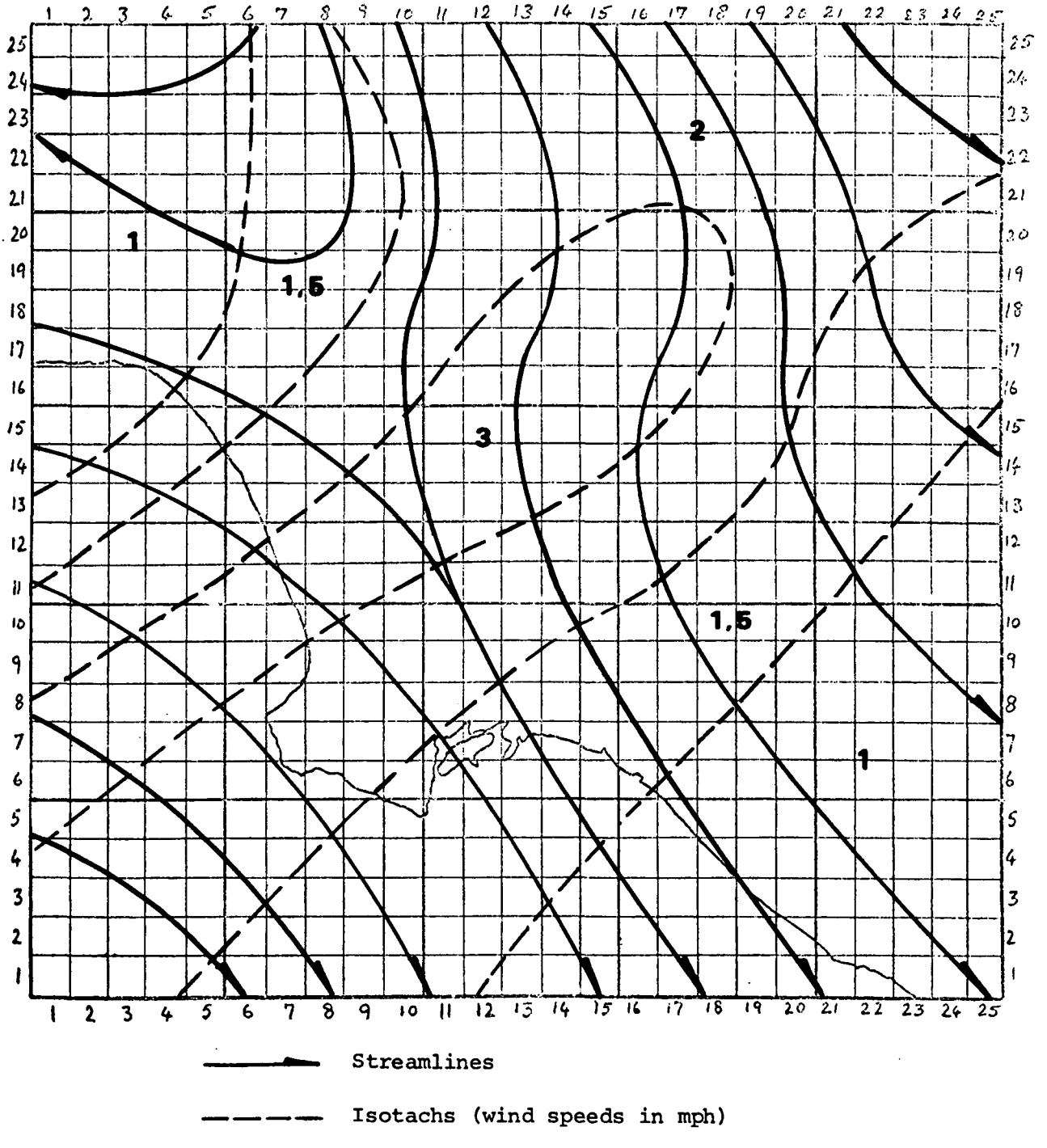

Figure 2. Modified Surface Wind Map for Los Angeles Basin (29 September 1969, 6:30-7:30 PST)

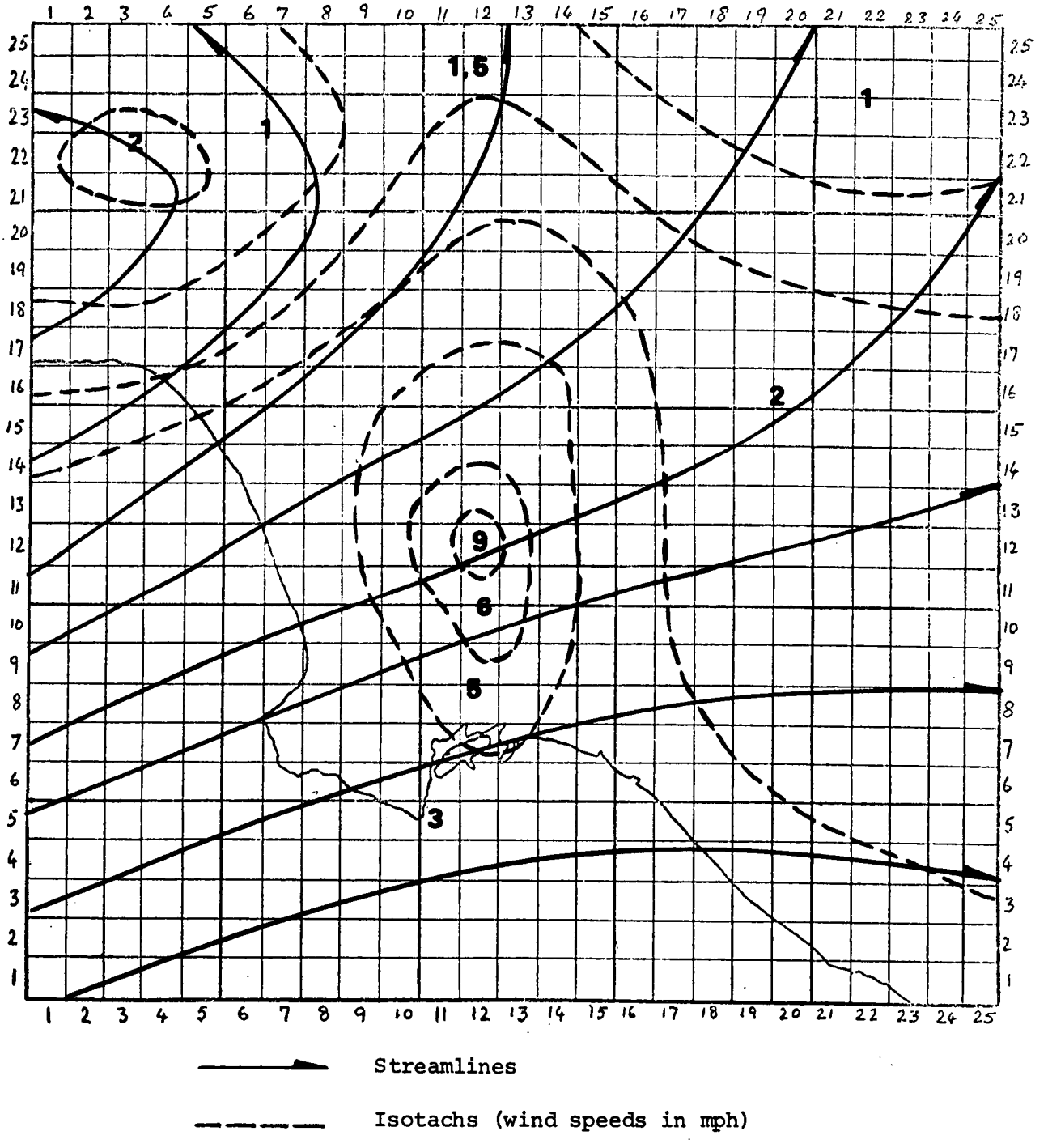

Figure 3. Modified Surface Wind Map for Los Angeles Basin (29 September 1969, 9:30-10:30 PST)

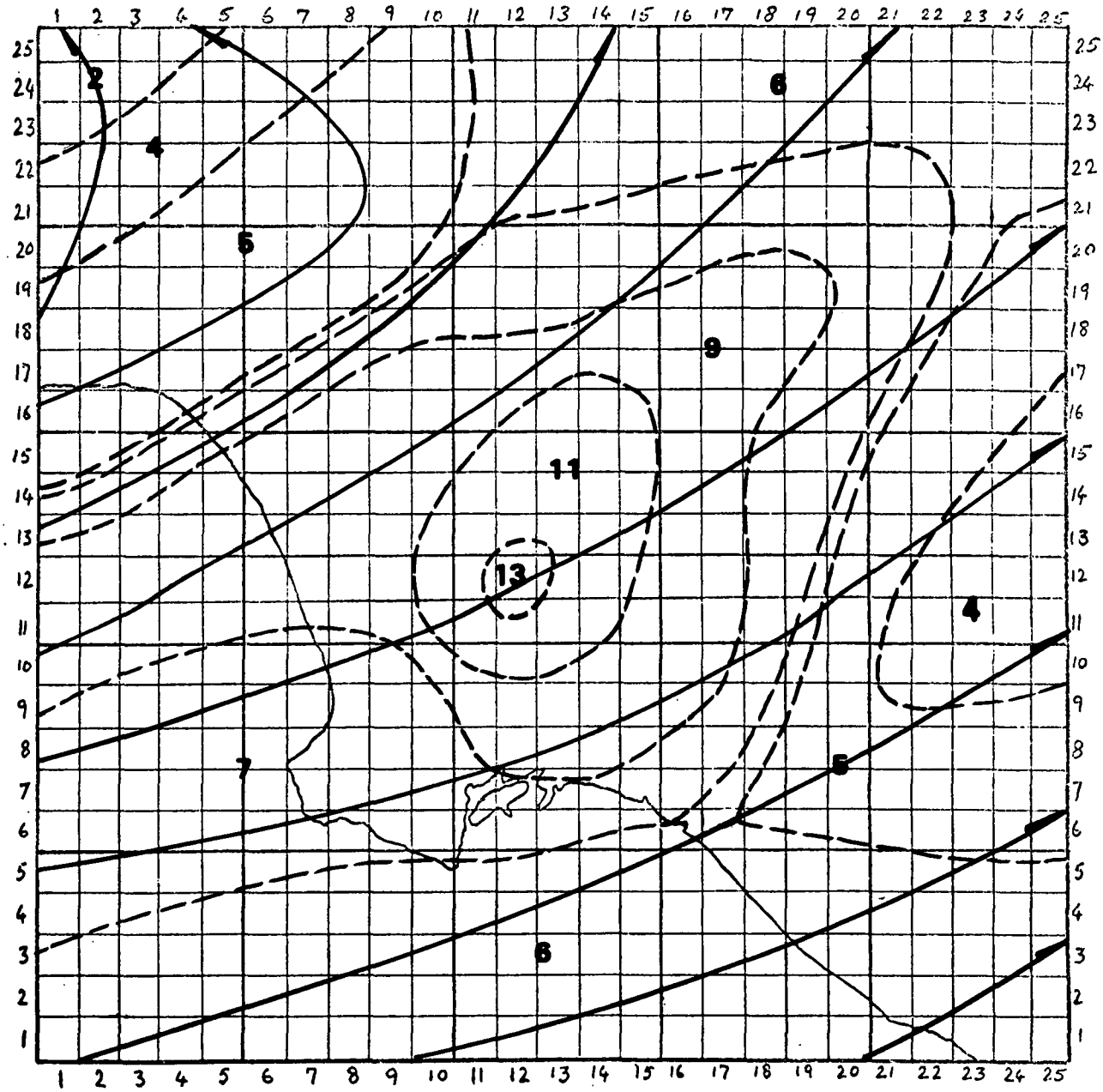

Figure 4. Modified Surface Wind Map for Los Angeles Basin (29 September 1969, 12:30-13:30 PST)

c. *Preparation of inversion maps.* On pages C-17 to C-21 of Roth et al. (1971), we have outlined an algorithm for the preparation of hourly maps of mixing depth. The basic variable in the algorithm is height of the inversion base, $H(x,y,t)$. However, the variable of interest is the mixing depth, that is, $H(x,y,t)$ less the terrain elevation, $h(x,y)$. If maps are prepared and smoothed using $H(x,y,t)$, $(H-h)$ as a function of x and y is an irregular, or "bumpy", surface. We have thus elected to prepare maps with $(H-h)$ as the basic variable, so that surfaces of mixing depth are reasonably smooth.

d. *Movement of the inversion with time.* In calculations carried out during Phase I, the height of the inversion base was held constant during the full hour over which it applied. When the inversion base was moved, new material (i.e., pollutants) was introduced at a concentration equal to that just below the inversion prior to its displacement upward. During the Phase II effort, we made the two changes in this procedure. First, we now move the inversion base at each time step, using linear interpolation between hourly maps to determine its vertical position at the location (x,y) . We believe that this procedure is more consistent with reality. Second, we introduce material through the rising inversion at a concentration determined according to the algorithm discussed in part 5d of this section (pages 35-36). This procedure was adopted as we believe that introduction of high concentration material beneath a rising inversion is probably inconsistent with actual behavior. Measurements indicate that contaminant concentrations aloft (with the exception of ozone) are generally lower than those specified using the original algorithm. Thus, the new procedure introduces pollutants beneath the inversion at concentrations that correspond more closely with those observed.

e. *Use of actual radiation intensity data.* In Appendix B of Roth et al. (1971) we presented curves representing the effect of the diurnal variations in solar intensity on the rate constants for the photolytic dissociation of NO_2 and HNO_2. These curves, however, are representative only for clear skies and in the absence of photochemically-generated haze. In the evaluation studies carried out in the current project, we used *actual* intensity data, as measured by Scott Research Laboratories at Commerce and El Monte for the six validation days. We present the curves used in the next section under evaluation Procedures.

4. Numerical Analysis

a. *Finite difference procedure.* We discovered early in the evaluation studies that, in employing the second and fourth-order differencing procedures given by Crowley (1968) and Fromm (1969) respectively (see Appendix D of Roth et al. (1971)), negative concentrations were generated on occasion in the vicinity of large concentration gradients. To eliminate the possibility of introducing this type of error, we have adopted a finite difference procedure described by Price, Varga, and Warren (1966). While this procedure is somewhat less accurate than the second order technique of Crowley, it is, of course, more accurate than a first order method. And the main purpose, elimination of negative concentrations, has been realized.

b. *Solution of the nonlinear difference equations in the* ρ *direction.* In Appendix D of Roth et al. (1971) we describe the method we have used for solving the nonlinear difference equations in the integration step in the ρ direction. In essence, the method is a simple iterative procedure that has displayed no convergence problems and has given consistently good results. During the current study we have experimented with the use of Newton's method (Isaacson and Keller, 1966) for solving the nonlinear equations. Test results indicated that this procedure is somewhat more accurate than

the method we have used previously. As a result, we have incorporated Newton's method into the operating program.

c. *Tests of accuracy.* We carried out four sets of computations to examine questions pertaining to the accuracy of the numerical procedure. Using the differencing algorithm of Price et al. (1966), we

(1) executed a simulation with no wind, no emissions fluxes, constant inversion height, and a uniform concentration field in order to evaluate the accuracy of the treatment of photochemistry in the airshed model. Predicted concentrations were compared with those generated using Gear's routine (1971) in integrating the coupled, first-order, ordinary differential equations that represent the photochemistry alone. (See Appendices B of Roth et al. (1971) and of this report for a discussion of Gear's method.) Predictions differed by no more than 2% between the two methods, confirming the validity of the treatment of photochemistry in the urban airshed model.

(2) compared predictions of the full airshed model under typical simulation conditions using time steps of various magnitudes. We found that predictions based on a one-minute time step differed only slightly from those based on a four-minute time step. This test confirmed that it is not necessary to restrict time steps to short intervals (1 minute or less).

Comments made thus far regarding numerical procedures are summaries of more complete discussions to be found in Appendix D of this report. Omitted from the Appendix D, however, are the results of two tests of the numerical procedure that were carried out prior to the adoption of the Price et al. differencing scheme. We present them here because we believe that the results are both of value and of general interest.

Early in the current study, using the Crowley and Fromm differencing procedures, we

(3) carried out a series of test runs for carbon monoxide to establish the merits of using numerical approximations of various orders. Using an initial concentration distribution based on 29 September data and simplified wind profiles, we found that truncation errors realized using first, second, and fourth order approximations are roughly in the ratio of about 2:1.5:1. These results clearly indicated that accuracy improved substantially with increasing order of approximation.

At the same time, as we discussed earlier, we observed the occasional occurrences of negative concentrations in areas of steep concentration gradients when second and fourth-order approximations were adopted. Searching for a means for eliminating these errors, we found the procedure suggested by Price et al., which is a second-order approximation. Unfortunately, we were unable to find a suitable fourth-order procedure. Confronted, then, with the choice of a second-order procedure and elimination of negative concentrations or a fourth-order procedure and the occurrence of negative concentrations, we selected the former. It is, of course, very much worthwhile to develop or locate a fourth-order procedure having the described properties.

(4) carried out two test runs to explore the relationship between the spatial resolution of the model and both the accuracy of the model and of the numerical integration procedure. The two test runs were made for the following conditions:

(a) Reduce grid size from 2 x 2 mile to 1 x 1 mile and integrate the equation of continuity for CO using the same emissions and meteorological data as in the simulation described in Roth et al. (1971). Assign one-fourth the traffic volume of each 2 x 2 mile grid square to the new 1 x 1 miles squares. It was the purpose of this run to explore the *accuracy of the numerical technique*. (The effect of a finite grid approximation on the numerical accuracy of a computation can be investigated in two ways. The first is to change the order of the finite difference approximation; this source of error was discussed earlier. The second way is to vary the grid size.)

(b) Assign the fraction of freeway emissions calculated for each 2 x 2 mile square to the appropriate new 1 x 1 mile squares, thereby increasing the spatial resolution of the automotive emissions inventory. The purpose of this run is to test the *accuracy of the model* with respect to major line sources of emissions by comparing results of the integration with those obtained in the first test.

Because of the relatively complex nature of the model and the associated emissions patterns, the tests were not expected to be definitive. However, we thought it preferable to carry out the runs under the actual modeling conditions, as fabricated conditions might be less revealing.

The two test runs were carried out for a 24 x 24 mile (or 12 x 12 grid square) test region, that included between rows 7 and 18 and columns 5 and 16 of the actual 50 x 50 mile modeling region. Comparisons of predictions with actual data were made for the West Los Angeles (WEST), Lennox (LENX), Commerce (COM), Long Beach (LONB), and downtown Los Angeles (CAP) locations. For the test run (a), predictions for each set of four 1 x 1 miles squares were averaged for hourly comparisons with predicted values computed on a 2 x 2 mile grid (and for comparison with the data). While no pattern of differences emerged, we observed that the average of the 4 - 1 x 1 mile values typically differed by no more than 1 or 2 ppm from the 2 x 2 mile grid predictions (only rounded integers are printed out). These results indicate how different the predictions might be if a smaller grid were used; they do not represent a true measure of accuracy. What we *can* conclude is, that in light of the minor changes in predicted values that were observed, the added cost associated with adopting a 1 x 1 mile grid system is a cost that is not worth incurring.

The results of test run (b) clearly demonstrate that the model is sensitive to the degree of resolution

employed in the treatment of freeways. Comparisons, in this case, were made between measured values and predicted values computed on the basis of the location of the monitoring station. If the station is located within a 1 x 1 mile square, the prediction for that square was used; if the station is located on a border between two 1 x 1 miles squares, the average of the predicted values is used. (We also noted the fraction of freeway emissions that was assignable to each of the 4 - 1 x 1 mile squares that comprise a 2 x 2 mile square.) In general, accuracy improves with increasing fineness of resolution, and increases or decreases in the magnitude of predicted concentrations correlate directly with the fraction of freeway traffic assigned to the 1 x 1 mile grid square that includes the monitoring station. However, as before, the degree of improvement in accuracy is not sufficient to justify the increased costs associated with the adoption of a finer grid. In fact, it is clear that an area-wide model cannot incorporate the needed resolution and remain practical; rather, a model having resolution of the order of a freeway width is the appropriate "tool" for dealing with the type of inaccuracies in prediction that are observed in the vicinity of a monitoring station adjacent to a freeway (see Appendix C).

5. The Model

a. *The size of the grid.* In the original formulation we adopted a grid of nodes for integration of the governing equations that was comprised of 625 (or 25 x 25) 2 mile x 2 mile squares. Furthermore, the space between the ground and the base of the inversion in the transformed coordinate system was divided into ten strata. In the current version of the model we have eliminated 198 of the 625 squares covering the 2500-square mile area, as these squares lie over the ocean and mountainous areas having no pollutant sources of consequence. Moreover, we found in carrying out CO evaluation runs that

predicted concentrations vary only slightly with large variations in the number of strata incorporated in the vertical. In particular, simulations involving five strata display concentration profiles that are only slightly flatter than those calculated using ten, and the differences in predicted concentrations at the ground are not significant. We thus reduced the number of vertical strata in the model to five. (Further reduction in number of strata may also be appropriate, subject to the results of additional sensitivity studies.)

b. *Form of the continuity equations.* We have adopted the conservative form of the continuity equations. Previously we have used a non-conservative form of the governing equations (D-1) of Roth et al. (1971), Appendix D, one given by Equations (D-4) of that report. The conservative form ensures that a material balance is maintained across all cell boundaries; the non-conservative (or advective) form does not (except for the case of uniform flow). The present equations are:

$$\frac{\partial(\Delta H c_i)}{\partial t} + \frac{\partial(u\Delta H c_i)}{\partial \xi} + \frac{\partial(v\Delta H c_i)}{\partial \eta} + \frac{\partial(W c_i)}{\partial \rho} = \frac{\partial}{\partial \xi}\left(K_H \Delta H \frac{\partial c_i}{\partial \xi}\right)$$

$$+ \frac{\partial}{\partial \eta}\left(K_H \Delta H \frac{\partial c_i}{\partial \eta}\right) + \frac{\partial}{\partial \rho}\left(\frac{K_V}{\Delta H}\frac{\partial c_i}{\partial \rho}\right) + R_i \Delta H + S_i \Delta H \qquad i=1,2,\ldots,N$$

The horizontal boundary conditions have been altered somewhat since horizontal diffusion is allowed in this formulation of the governing equations.

c. *Form of the transformed equations.* The transformed equations now include horizontal turbulent diffusion. While horizontal diffusion is generally unimportant in a model of a two-mile spatial resolution, the model can now be applied when the spatial grid is much finer, and thus when the effects of horizontal diffusion may be significant.

d. *Treatment of the boundary conditions at the inversion base.* In order to specify the concentration of pollutants that enter the modeling region as the inversion rises, we must,

in the absence of concentration data aloft, make some assumption as to the nature of the vertical concentration distribution. Thus, at the beginning of a simulation ($t=t_o$), we establish the following concentration distribution aloft over each grid square:

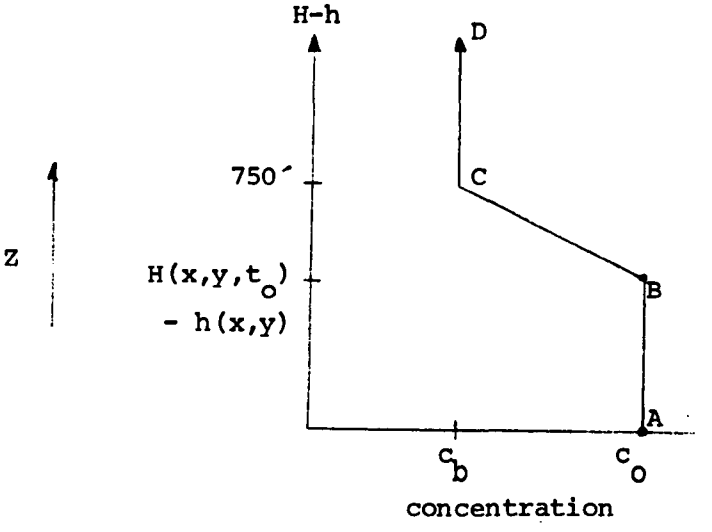

where

c_o = initial concentration in the column of grid cells above a particular grid square.

c_b = assumed background concentration aloft above the grid square.

$H(x,y,t_o)$ = height of the inversion base at t_o and location (x,y).

$h(x,y)$ = terrain elevation at (x,y).

In the profile shown, $\overline{AB}$ denotes the initial condition, and $\overline{BCD}$ denotes the assumed concentration profile aloft (above the inversion base). As the base of the inversion rises, the concentration of pollutant in the air engulfed is given by the location of the height of the inversion base and the corresponding concentration on the segment $\overline{BCD}$. A profile is constructed for all species except ozone. In the case of this pollutant we calculate the concentration at the boundary through use of the steady-state approximation involving HC, NO, and NO_2.

e. *Development of a two-dimensional version of the model.* We prepared a two-dimensional version of the airshed model for use in the initial phases of model implementation and testing. As vertical gradients in concentrations were found to be small and the cost of operating a three-dimensional model is considerable, use of the two-dimensional formulation served as an inexpensive means for carrying out tests involving numerical procedures, treatment of the chemistry, etc. We were also able to compare predicted concentrations using both the two- and three-dimensional models to determine if, in fact, a three-dimensional formulation, with its additional complexity, was needed. While the differences in prediction were generally (though not always) rather small, we elected to carry through with the three-dimensional version. We recommend, however, that the question of dimensionality be further explored in future studies of model sensitivity.

6. Modeling of Subgrid Scale Phenomena

a. *Development of a microscale model for predicting concentrations of carbon monoxide in the vicinity of roadways.* Evaluation of a model having two-mile resolution is at best a questionable undertaking if available data are based on samples collected at a point. As an example, consider carbon monoxide emissions from automobiles in the vicinity of a monitoring station. Clearly, these emissions can influence measured concentrations at the station. In other words, the measurements are not necessarily (and are in fact unlikely to be) representative of the two-mile square in which the station lies if the station is adjacent to a major roadway (which is generally the case in Los Angeles). In an initial and limited study to examine the utility of combining regional and subgrid scale models to resolve problems in validation attributable to mismatches in scale, we developed a microscale model for describing the contribution of local vehicular sources to pollutant concentrations measured at monitoring stations. This work is fully described in Appendix C of this report.

b. *Revision of the power plant emissions model.* During the current effort we made a number of revisions to the power plant emissions model described in Appendix A of Roth et al. (1971), particularly with regard to

- the apportionment of emissions from a power plant among cells downwind of the source
- the inclusion of temporal variations in emissions rates
- the treatment of "inversion penetration"
- the calculation of the average molecular weight of emitted hydrocarbons.

These modifications are discussed in Appendix A of this report.

7. Computer Programs

a. *Emissions calculations.* In Appendix F of Roth et al. (1971) we referred to an Aircraft Emissions Program. We have taken that part of the Aircraft Emissions Program used to calculate emissions from ground operations and included it in the newly-created Emissions Data Preparation Program. In addition, all ground level emissions are now calculated in this program and written on tape (or disc) for input to the Atmospheric Pollution Simulation Program (APSP). Thus, emissions from all sources, with the exception of power plants, are input to the APSP from tape (or disc). The APSP has been altered to the extent necessary to incorporate the changes.

b. *Plotting of concentration profiles.* As a part of the current effort, we have developed a program for plotting predicted concentration-time profiles (concentrations being hourly averages) for all pollutants for which time histories are computed [CO, hydrocarbon (inert, reactive, and total), NO, NO_2, and O_3]. Experimental results, urban scale model predictions, and micro-model corrections can all be displayed. These plots serve as the main mode of presentation of data and predictions in Section III of this report.

In addition to these changes, we have made a number of improvements in input and output procedures, attempting to maintain both simplicity and generality. One result is that total printed output of a simulation has been reduced by more than 50%. We have also "streamlined" the program to eliminate unnecessary calculations, particularly those introduced for evaluative or comparative purposes at an earlier stage of model development. Finally, we have made it considerably easier to make alterations in the photochemical kinetics mechanism, should such changes prove necessary in the future. The complete set of programs comprising the urban airshed model is described in Volume II of this report.

8. Air Quality Data

In Appendix E of the Roth et al. (1971) we discussed in some detail the air quality data used in model evaluation. We have since reviewed the air quality measurement techniques employed by the APCD in terms of accuracy, specificity, and reliability, and we make the following observations. First, accuracies are, in general, no better than $\pm$ 10% in the determination of pollutant concentrations (for any pollutant), and degree of specificity and reliability varies greatly, depending upon the measurement. Second, corrections to measurements must be made for certain pollutants. These are as follows:

CO	No correction needed.
NO	The oxidation of NO to NO_2 prior to colorimetric measurement of the product NO_2 is 70 to 85% efficient. Thus, reported NO concentrations must be increased by about 20% for use in validation.
NO_2	PAN interferes with measurement of NO_2. Accuracy of measurement is ±10 to 20%. No correction is recommended, however, due to lack of information--knowledge of PAN concentration and other sources of uncertainty.

oxidant — Presence of NO_2 increases oxidant readings by 10 to 20% of the NO_2 concentration; SO_2 decreases readings by an amount approximately equal to the SO_2 concentration. In Los Angeles, NO_2 will be the most significant interferent, although SO_2 will have a substantial effect in the southwest portion of the Basin. We correct for these interferences when they are significant.

total hydrocarbons — Flame ionization is specific for carbon, recording oxygenated hydrocarbons as well as hydrocarbons. Readings are difficult to interpret because

(a) Calibration is carried out using a specific hydrocarbon (APCD uses methane), whereas the hydrocarbons measured are a complex mixture. While it is assumed that response is proportional to the number of carbon atoms, significant deviations from this assumption have been observed.

(b) Methane is by far the dominant constituent, making determination of nonmethane constituents by difference a highly uncertain matter.

(c) Variation in reactivity with type of HC affects measurement.

We have thus concluded that these measurements are too uncertain to be of much value.

In summary, CO and NO_2 concentrations are used as reported, whereas NO and oxidant are "corrected" in the manner indicated. Total hydrocarbon measurements are considered to be of little value.

In applying these corrections, we have made the following exceptions:

- At Commerce and El Monte, the NO and O_3 measurements made by Scott were not corrected, as they were made using procedures that do not require a correction.

- At Long Beach, oxidant measurements were not corrected for SO_2 or NO_2 interference due to the uncertainty inherent in applying the correction when the interferents are present in high concentrations relative to the species being measured.

III. EVALUATION OF THE MODEL

Evaluation of the urban airshed model consists of integrating the governing equations and comparing predicted concentrations with those measured at local air quality monitoring stations. Evaluation was undertaken in the following sequence for each of six days in 1969, days for which a rich data base was available.

1. Evaluation for carbon monoxide. Exercise of the model for an inert species such as CO provides a basis for evaluating the treatment of meteorological variables. Validation for CO, of course, also constitutes a test of most aspects of the numerical integration technique and of portions of the source emissions inventory.

2. Evaluation for total hydrocarbon, nitrogen oxides, and ozone. Upon successful completion of 1., and upon the incorporating modifications suggested by the results of the validation for CO, Evaluation of the airshed model for reactive species may proceed.

It is the purpose of this section to describe the evaluation procedure, to present the results of the evaluation effort, and to examine and discuss these results.

Failure in validation suggests inadequacy of the model, inaccuracies in the meteorological and/or emissions data that are inputs to the model, and/or inaccuracies in the observed concentrations. While it is clear that deficiencies in the emissions, meteorological, and air quality data can only serve to enhance discrepancies between prediction and measurement, the impact on evaluation of shortcomings in the model requires some examination. In particular, we wish to focus on a problem inherent in the evaluation of any airshed model in which quantities are spatially averaged -- the comparison of "point" measurements with spatially averaged predictions.

Consider the evaluation of the urban airshed model, where carbon monoxide is the pollutant of concern. The model is based on the assumption that emissions are uniformly distributed in space and time (over an hourly interval) over each 2 x 2 mile cell and that meteorological conditions are also invariant over this scale. The direct result of these assumptions is that *the predicted pollutant concentrations* are uniform within each grid square (or cell). *The observed values* of CO, however, typically are representative only of the CO concentrations in the immediate vicinity of the monitoring station. Of the ten monitoring stations operated by the Los Angeles County APCD, seven are located within 100 feet of a roadway having a daily traffic count in excess of 15,000 vehicles. Ott (1971) has shown that CO concentrations measured at a monitoring station situated along a busy city street are approximately twice the background level (400 feet or more away from the street) and slightly more than half that measured at

the sidewalk located between the street and the station. Thus, while we may expect that a properly formulated urban scale model will predict background levels of CO with reasonable accuracy on a 2 x 2 mile scale, there is no justification for comparing these predictions with local point observations. In the discussion that follows we refer to the inappropriateness of comparing predicted and measured concentrations as "the problem of disparate scales".

The magnitude of the problem of disparate scales varies with the type of pollutant being considered. As automobiles are the major source of hydrocarbons and nitrogen oxides, as well as of carbon monoxide direct comparison of prediction and measurement for these pollutants is also invalid. Hydrocarbons and NO_x, however, participate in photochemical reactions, and, as a result, the impact of local emissions on measurements is more complex than in the case of CO. Ozone, for example, reacts with nitric oxide (rapidly, of course, when concentrations are high), thus reducing the concentration of both species in the vicinity of source, and thus, in Los Angeles, often in the vicinity of monitoring stations.

In carrying out the evaluation studies reported here, we plainly had to accept the fact that, while we wished to have area-averaged measurements, only "point" measurements were available. However, resolution of the problem may be effected not only by obtaining area-wide averages, but also by developing a model capable of predicting local elevations in concentration that are due to emissions from nearby sources. With this need in mind we undertook a limited effort to develop such a model. The model is applicable only for carbon monoxide and was used for validation in the vicinity of only four monitoring stations. While the results are promising, it must be emphasized that the development study was, in effect, mainly a pilot study carried out to determine if the development and application of the model represented a flexible means for resolving the problem of disparate scales. The developmental work and the results are fully described in Appendix C. The estimated contributions to measured concentrations made by local sources at the four stations (as predicted by the subgrid scale model) are shown in results presented later in this section.

In closing this discussion, we wish to emphasize that the problem of disparate scales is perhaps the major barrier to satisfactorily assessing the performance of urban scale models. Its lack of resolution has had a detrimental effect on this work and will continue to be an issue until spatially averaged measurements are made, or subgrid scale models are developed.

A. The Evaluation Procedure

As we have noted, evaluation of the airshed simulation model for a particular "validation day" consists of a sequential procedure, evaluation for carbon monoxide followed by evaluation for nitrogen oxides, hydrocarbons, and ozone. The steps involved are the following:

1. *Preparation of meteorological and emissions data.* Hourly wind speed, wind direction, and mixing depth maps are prepared for each

validation day, as described in Appendix C of Roth et al (1971) and in Section IIC of this report. As it is assumed that the emissions inventory is applicable for all weekdays in 1969 and as all validation days are weekdays, we use the inventory without alteration, as reported in Appendix A of Roth et al (1971) and Appendix A of this report.

2. *Preparation of other inputs to the model specific to the validation day.* These include:

   a. *Initial conditions.* Initial concentrations are specified in each ground level grid cell by interpolation using the data collected at monitoring stations during the hour at which solution is initiated. Maps are needed for CO, NO, NO_2, and reactive and unreactive hydrocarbon (RHC and UHC). Initial ozone concentrations are calculated assuming that the rate of reaction of ozone is equal to zero. (Thus, the initial O_3 concentration is given by an algebraic expression involving initial RHC, NO, and NO_2 concentrations.) Initial concentrations in cells aloft are set equal to the concentration in the ground level cell.

   b. *Boundary conditions.* Boundary concentrations must be specified for each hour for all grid cells that lie along an inflow boundary from the ground to the inversion base. Also, concentrations must be specified along the upper boundary (the base of the inversion) when there is an influx of material from above the inversion. The horizontal boundary conditions (east, west, north, and south boundaries, where the winds enter the modeling region) are established by using the concentrations measured at the nearest monitoring station at the hour in question as a guide. Variations in concentrations with x and y along the boundary at a given t in regions remote from monitoring stations are estimated solely on a judgmental basis. It is assumed that concentration is invariant with z for a given x, y, and t. Boundary conditions aloft (at the inversion base) are established for a particular day, as described in Section IIC of this report. As with initial conditions, boundary concentrations of ozone are computed assuming that the rate of reaction of ozone is zero.

   c. *Radiation intensity data.* Actual measurements of radiation intensity at the ground as a function of time were made by Scott Research Laboratories at El Monte and Commerce for the validation days. The measured curves (I vs. t) were corrected for variations in solar zenith angle (from tables prepared by the Dept. of Meteorology, UCLA (1966)) and normalized. The results, plots of $\{I \sec(z)/[I \sec(z)]_{max}\}$ vs. t for each of the validation days are given in Figures 5 through 10. Averages of the normalized, angle-corrected intensity measurements made at the two stations are then related to k_1 through

the relationship given in Figure 11, as reported by Eschenroeder and Martinez (1970).

d. *Rate constants and stoichiometric coefficients for hydrocarbon reactions.* Referring to the kinetic mechanism presented in Appendix C, the following parameters must be established: k_{11}, k_{12}, k_{13}, k_{15}, α, β, δ, and ε. To do this, we lumped reactive hydrocarbons into four groupings--paraffins (excluding methane, ethane, and propane), aromatics (excluding benzene), ethylene, and olefins (other than ethylene). Taking n-butane to be representative of the paraffins, toluene of the aromatics, and propylene of the olefins, we computed lumped rate constants for the HC-O, HC-OH, HC-ozone, and PAN formation reactions based on weighted averages of the individual rate constants established during evaluation of the kinetic mechanism. The weights are taken as the proportion of each group (paraffins, aromatics, etc.) present in the atmosphere.

Gas chromatographic data collected by Scott Research Laboratories at Commerce and El Monte on the validation days were used in determining the averaged parameters. As there was little variation in composition with time of day, daily averages were calculated. Moreover, as the daily averages varied little from day to day, at least for the three days for which they were computed (29 September, 30 September, and 4 November), we used the individual averages for each of the three days (see Table 3) and the 29 September values for the remaining three days. Stoichiometric coefficients were calculated in a manner similar to that used for the estimation of the lumped rate constants.

The formulas used to calculate the various parameters are as follows:

$$\bar{k}_{ij} = \frac{\sum_i c_i k_{ij}}{\sum_i c_i}$$

$$\bar{\varepsilon} = \frac{\sum_i c_i \varepsilon_i}{\sum_i c_i}$$

$$\bar{\alpha} = \frac{\sum_i \alpha_i c_i k_{i,11}}{\bar{k}_{11} \sum_i c_i}$$

i = 1 paraffins
2 aromatics
3 ethylene
4 olefins

j = 11, 12, 13, 15
(j corresponds to the reaction number in Table 1 of Appendix B)

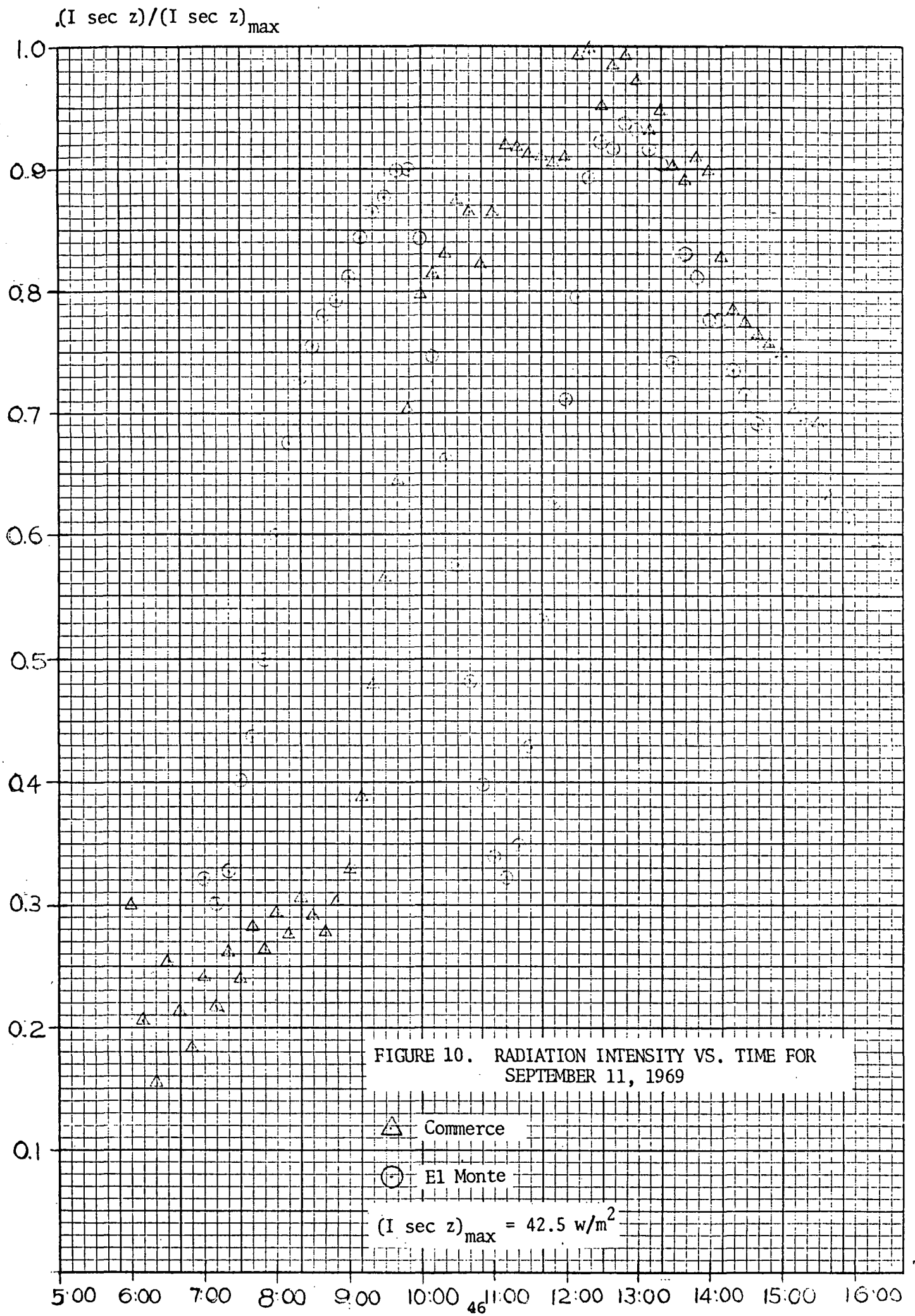

FIGURE 10. RADIATION INTENSITY VS. TIME FOR SEPTEMBER 11, 1969

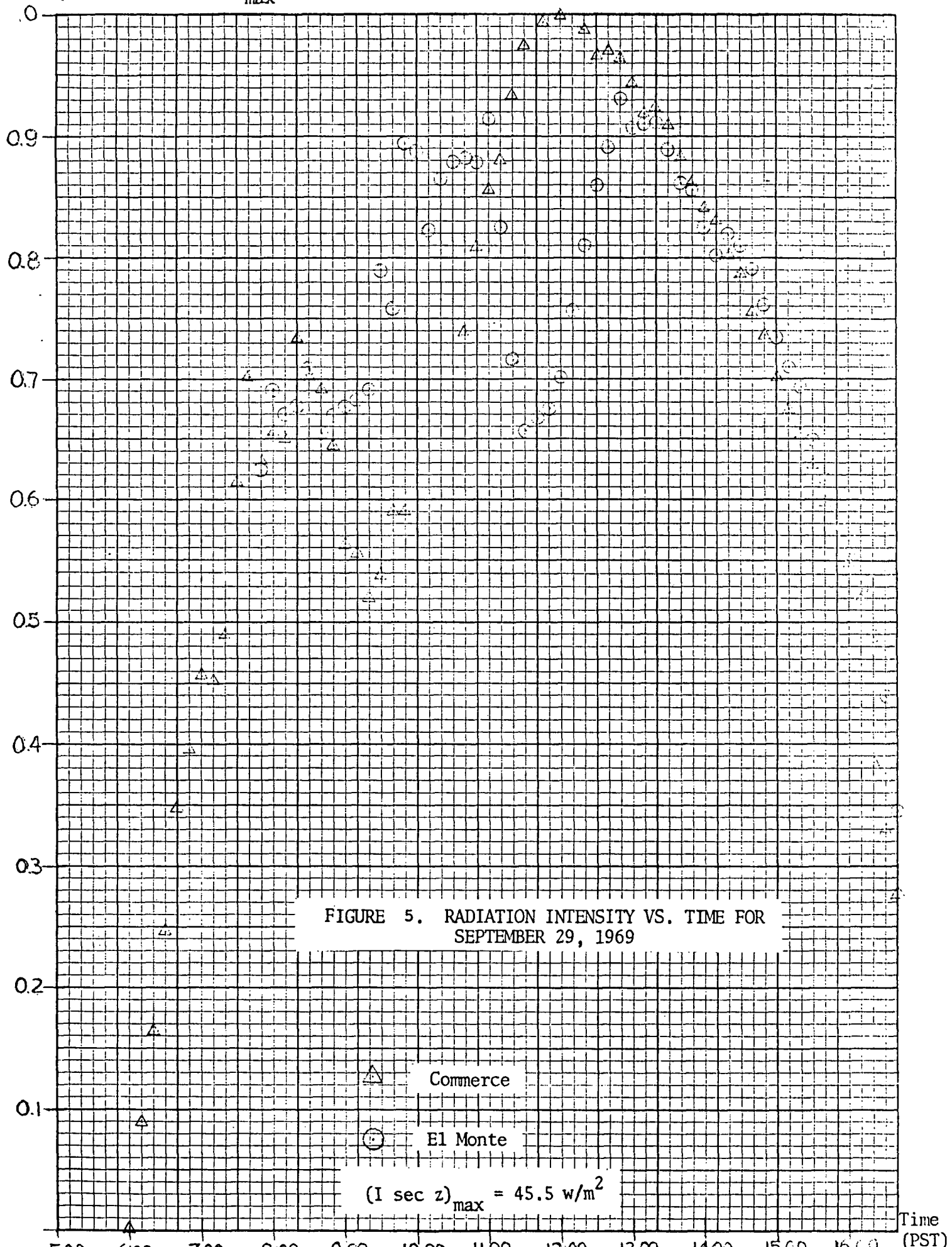

FIGURE 5. RADIATION INTENSITY VS. TIME FOR SEPTEMBER 29, 1969

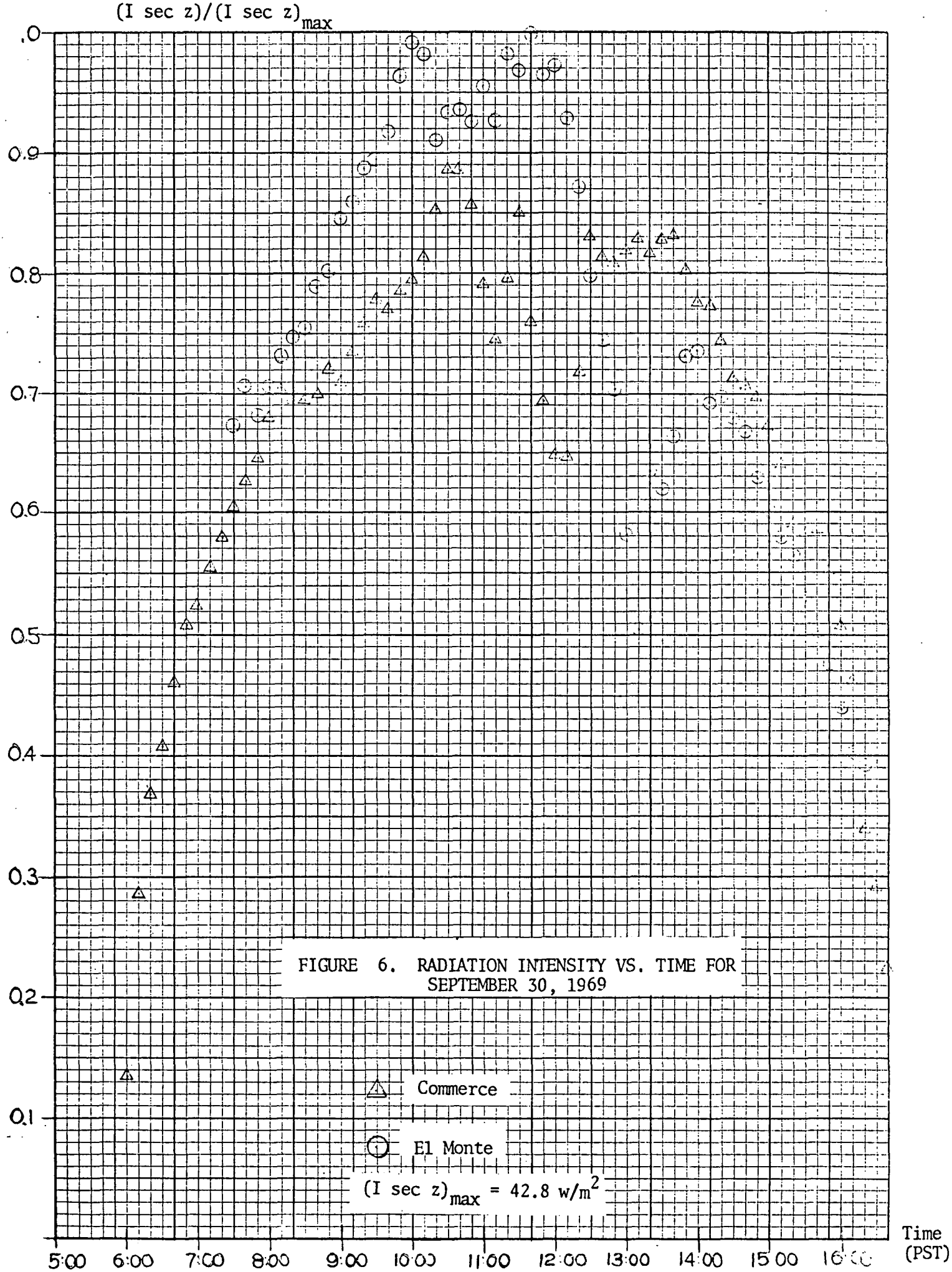

FIGURE 6. RADIATION INTENSITY VS. TIME FOR SEPTEMBER 30, 1969

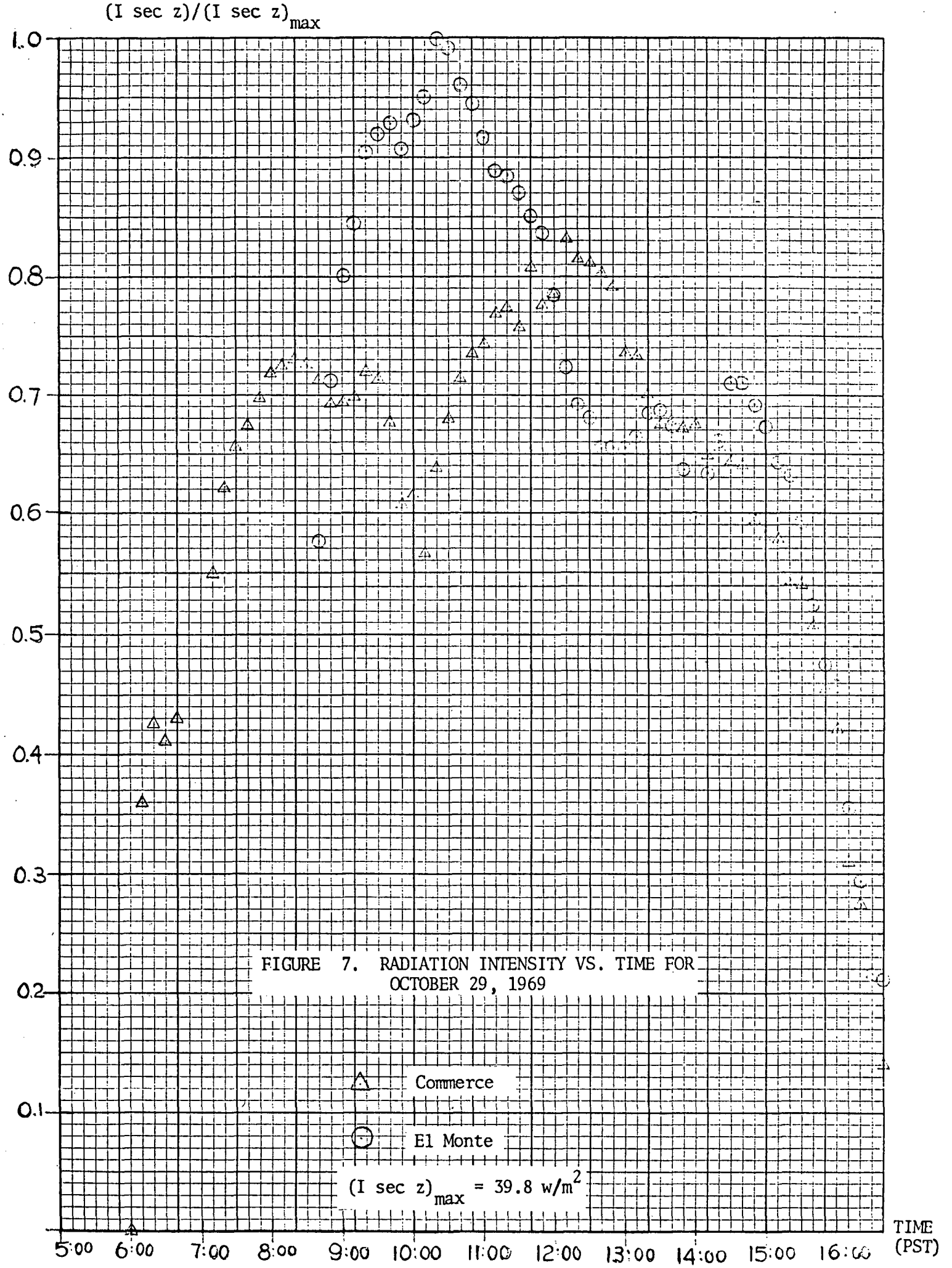

FIGURE 7. RADIATION INTENSITY VS. TIME FOR OCTOBER 29, 1969

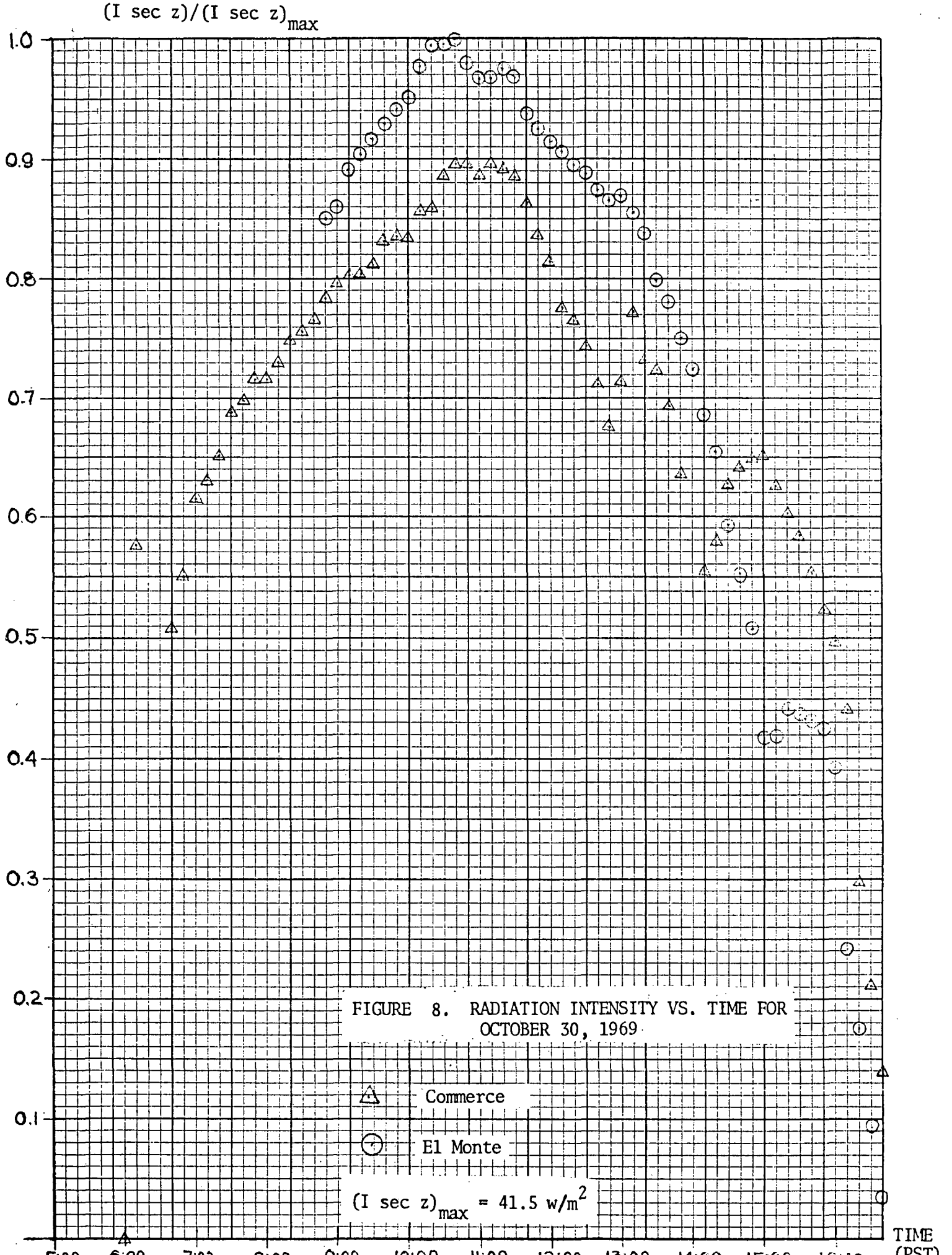

FIGURE 8. RADIATION INTENSITY VS. TIME FOR OCTOBER 30, 1969

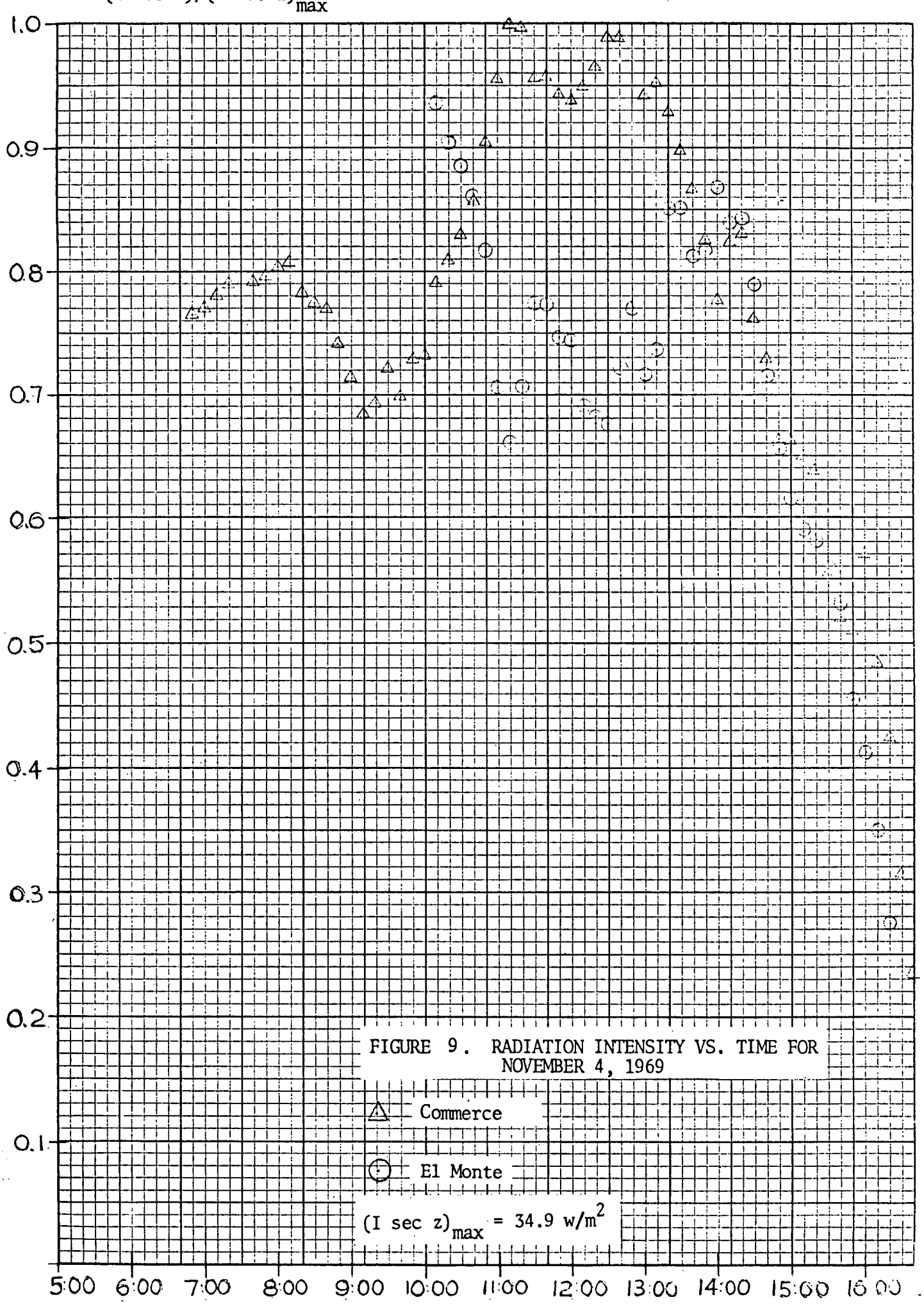

FIGURE 9. RADIATION INTENSITY VS. TIME FOR NOVEMBER 4, 1969

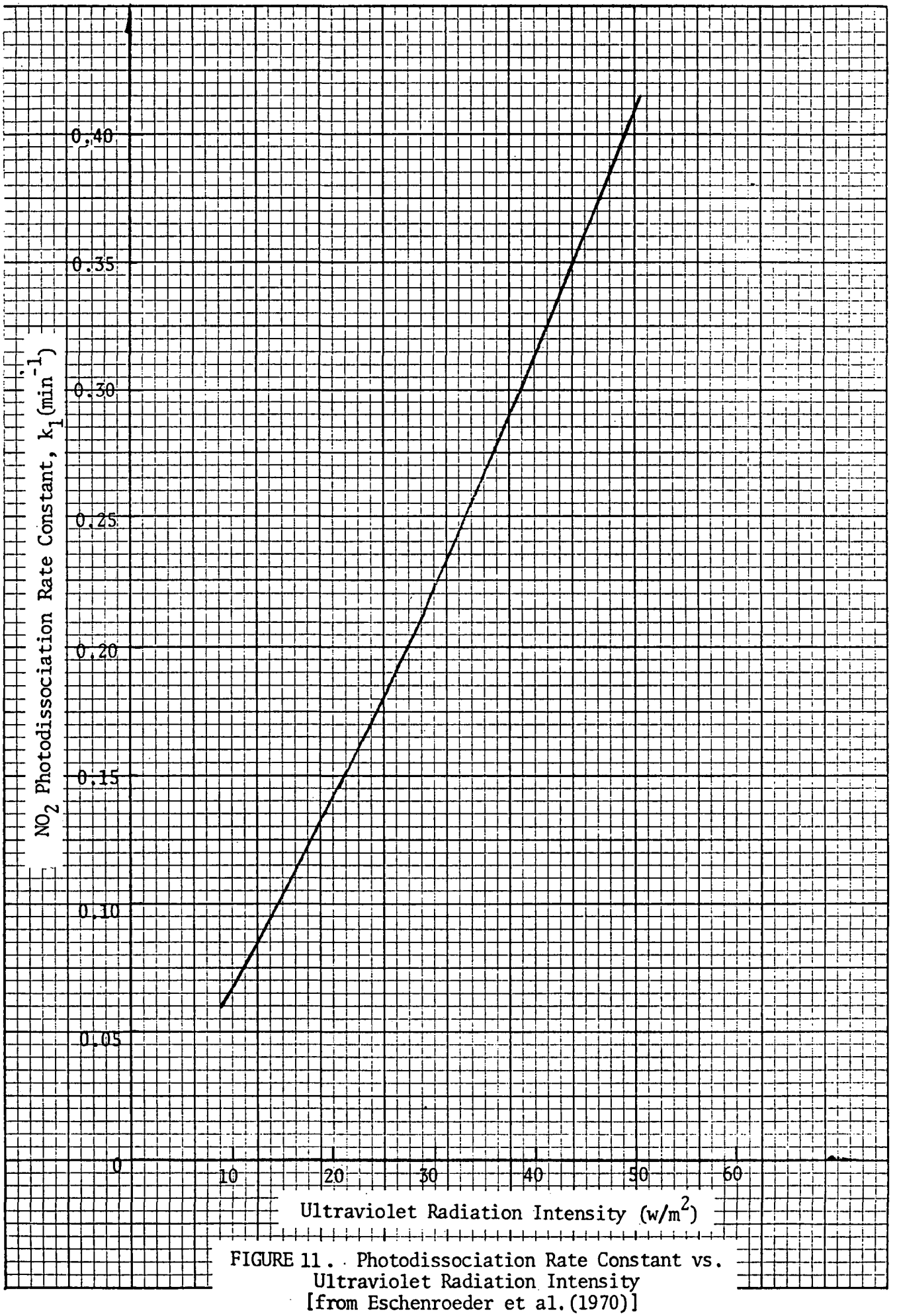

FIGURE 11. Photodissociation Rate Constant vs. Ultraviolet Radiation Intensity [from Eschenroeder et al.(1970)]

$$\bar{\beta} = \frac{\sum \beta_i \, c_i \, k_{i,12}}{\bar{k}_{12} \sum_i c_i}$$

Parameter values used in the calculation are summarized in Table 2, and values of the various parameters calculated for the three days are given in Table 3. The rate constants for inorganic reactions may be found in Appendix B.

3. *Evaluation for carbon monoxide.* The airshed model is exercised from 5 AM to 3 PM for each of the validation days. Predicted elevations in concentration in the vicinity of four monitoring stations due to local emissions (as given in Appendix C) are added to the airshed model predictions. Alterations were made in the 29 September and 30 September wind fields after initial simulations were carried out for these days. No other changes in input were made for these days, nor were any changes made for the four additional days. Hourly averages of predicted concentrations were computed (averages of concentration at each node computed for all time steps falling within the hours), with predictions rounded to the nearest ppm.

4. *Evaluation for nitrogen oxides, hydrocarbons, and ozone.* Upon satisfactory completion of the carbon monoxide simulation for a particular day, evaluation was carried out for the reactive species. All procedures are as described for CO. Results are rounded to the nearest pphm.

Comparison of predictions with measured values are made at the sites shown in Figure 12 and listed in Table 4. Since monitoring stations are not, in general, situated near the center of a ground level grid cell, we employ an interpolation procedure to calculate the predicted station concentration. In Figure 13, we illustrate the computations involved.

The ratio of simulated to computing time for the validation runs are as follows (IBM 370/155):

CO	150:1
NO, NO_2, RHC, UHC, and O_3 (as well as CO)	8:1

B. The Results

Evaluation was carried out for carbon monoxide (CO), nitric oxide (NO), nitrogen dioxide (NO_2), reactive plus unreactive (or total) hydrocarbon (HC), and ozone (O_3) for the ten hour period 5 AM to 3 PM for the following days in 1969:

11 September
29 September
30 September
29 October
30 October
4 November

TABLE 2 RATE CONSTANTS AND STOICHIOMETRIC COEFFICIENTS USED IN COMPUTING LUMPED PARAMETERS

	$k_{i,11}$	$k_{i,12}$	$k_{i,13}$	$k_{i,15}$	α_i	β_i	δ_i	ε_i
Paraffins (except methane, ethane, propane)	1,920	5,720	1.125×10^{-4}	9	5	1.2	4	.61
Aromatics (except benzene)	6,420	15,000	7.5×10^{-5}	30	6	1.2	4	.61
Ethylene	7,720	2,500	2.87×10^{-3}	3	16	0.2	4	.22
Olefins (except ethylene)	40,000	25,000	1.65×10^{-2}	3	16	0.2	4	.22

All reaction rate constants are in ppm^{-1} min^{-1}.

TABLE 3. COMPUTED VALUES OF THE RATE CONSTANTS AND STOICHIOMETRIC COEFFICIENTS FOR THREE OF THE VALIDATION DAYS

	29 September	30 September	4 November
$\bar{k}_{11}$	7,300	6,300	6,500
$\bar{k}_{12}$	9,500	8,400	8,000
$\bar{k}_{13}$	1.9×10^{-3}	1.7×10^{-3}	1.8×10^{-3}
$\bar{k}_{15}$	13.8	11.9	11.1
α	12	11.9	12.4
β	.95	.95	.92
δ	4	4	4
ε	.51	.52	.50

All computed parameters are rounded to either two or three significant figures.

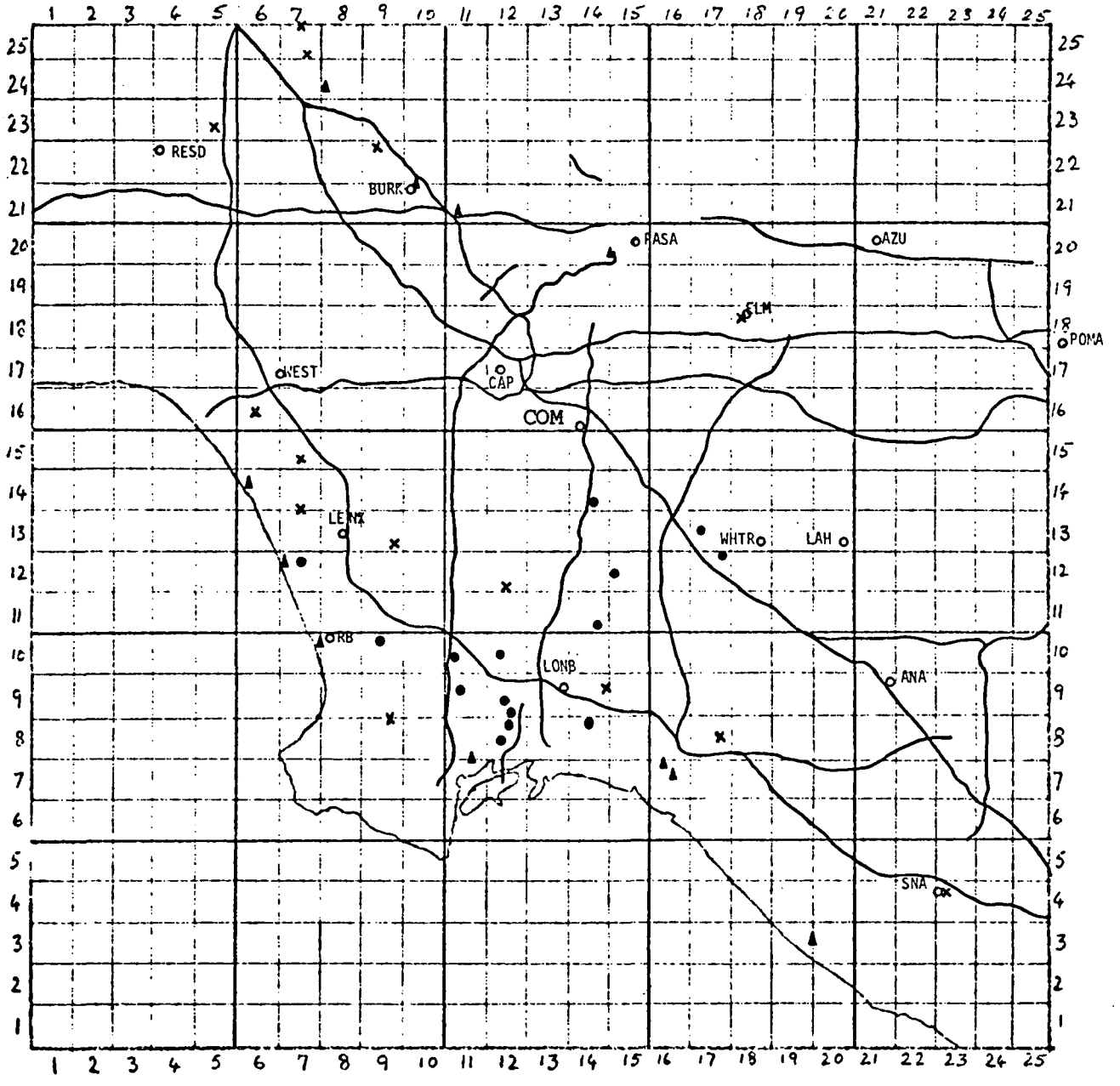

Figure 12. Locations of Monitoring Stations Relative to Major Contaminant Sources in the Los Angeles Basin

- ~ - freeways
- • - oil refineries
- ▲ - power plants
- x - airports
- o - contaminant monitoring stations

Table 4. Addresses and Locations of Contaminant Monitoring Stations in the Los Angeles Basin

Station Number	Station Code Name	Address
1	CAP	434 S. San Pedro Street, Los Angeles (at 4th Street)
60	AZU	803 N. Loren Avenue, Azusa (two blocks north of Foothill Boulevard)
69	BURK	228 W. Palm Avenue, Burbank (at Victory Boulevard)
71	WEST	2351 Westwood Boulevard, Los Angeles (1/2 block north of Pico Boulevard)
72	LONB	3648 N. Long Beach Boulevard, Long Beach (at 36th Street)
74	RESD	18330 Gault Street, Reseda (at Etiwanda Avenue)
75	POMA	924 N. Garey Avenue, Pomona (at Kingsley Street)
76	LENX	11408 La Cienega Boulevard, Los Angeles (at Imperial Boulevard)
78	RB	615 E. Anita Street, Redondo Beach (at Pacific Coast Highway)
79	PASA	1201 E. California Boulevard, Pasadena (at Wilson Avenue)
80	WHTR	14427 Leffingwell Road, Whittier (at Telegraph Road)
OC1	ANA	1010 S. Harbor Boulevard, Anaheim (at Vermont Avenue)
OC2	SNA	Paulorino Avenue, Near Airport Control Tower, Orange County Airport, Santa Ana
OC3	LAH	621 Ocean Avenue, La Habra (at Walnut Street)
Scott Research	ELM	El Monte Airport.
	COM	4545 E. Washington Boulevard, City of Commerce (at Long Beach Freeway)

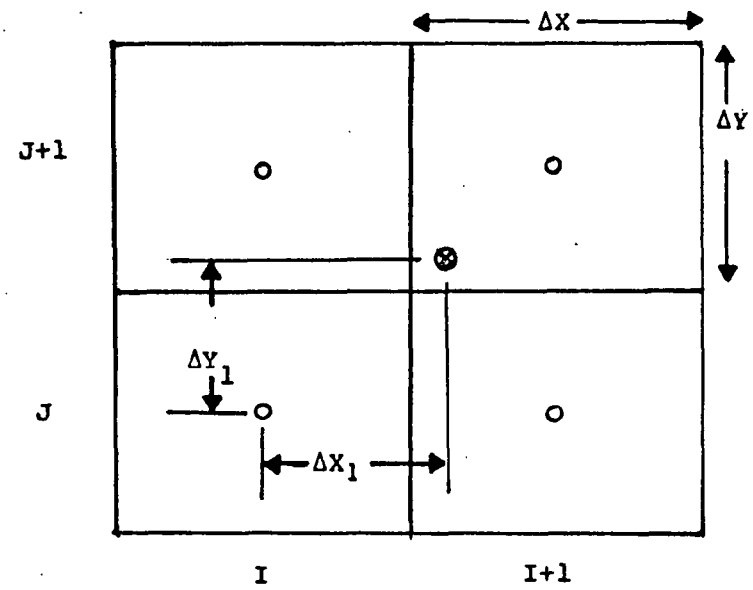

⊗ - monitoring station location

$$C_{station} = \left[C_{I,J}(1-\xi) + C_{I+1,J}\,\xi\right](1-\eta) + \left[C_{I,J+1}(1-\xi) + C_{I+1,J+1}\xi\right]\eta$$

where

$$\xi = \frac{\Delta X_1}{\Delta X}$$

$$\eta = \frac{\Delta Y_1}{\Delta Y}$$

$C_{I,J}$ = predicted ground level concentration above grid square (I,J)

$C_{station}$ = predicted concentration at the monitoring station

FIGURE 13. INTERPOLATION PROCEDURE FOR CALCULATING THE PREDICTED CONCENTRATION AT A MONITORING STATION.

The results are presented as computer plots of concentration vs. time for each pollutant at those stations and on those days when data were available. As there are five pollutants, fifteen monitoring stations, and six validation days, a large number of plots is required. (However, since NO and NO_2 are plotted together, since hydrocarbon is measured at a maximum of six stations, and since plots were usually prepared only when data were available, many fewer than 15x6x5 plots were needed.) Tables 5 to 7 indicate the pollutant/station/day combinations for which plots were prepared. The plots may be found at the end of this report, following the text.

Predictions of pollutant concentrations are also displayed on maps in grid form, that is, as a function of x and y (or for the grid square designated by (x,y)). Grid plots are generated for each pollutant (1) at each time step and (2) at hourly intervals (i.e., hourly averages). Examples of plots exhibiting hourly averages for the period 11 AM to noon on 29 September are given in Figures 14 to 19. Similar plots have been prepared, at individual time steps and as hourly averages, for all pollutants for all six validation days. However, we have not included them here.

Air quality data for 29 September and 30 September are described in detail in Appendix E of Roth et al. (1971). Data for the remaining four days were supplied to us by EPA. Most of the air quality data were collected by the Los Angeles and Orange County Air Pollution Control Districts which together operate a total of thirteen monitoring stations in the modeling region. However, as we have mentioned earlier, Scott Research Laboratories collected air quality data at two additional sites during this period. We refer the reader to their report, "1969 Atmospheric Reaction Studies in the Los Angeles Basin", Vol. I-IV (1970), describing the data collection program.

Air quality data are corrected in accordance with the procedures described in Section IIC and are displayed in the Figures in corrected form. Special attention, however, must be given to the comparative presentation of hydrocarbon concentrations. Total hydrocarbon measurements were made on a regular basis at four locations in the Basin--Downtown L.A., Azusa, Pasadena, and Anaheim. Methane is monitored at three of these stations, the exception being Anaheim. In addition, Scott Research Laboratories measured hydrocarbons using both flame ionization and gas chromatographic methods at El Monte and Commerce. As we treat unreactive (U) and reactive (R) hydrocarbons separately in our model, measured and predicted concentrations must be placed on the same basis for the purpose of comparison.

As most data are reported as ppm carbon (ppm C), we have converted predicted hydrocarbon concentrations, for both reactive and unreactive groupings, to ppm C in the following manner. For the Scott GC measurements, we have computed the average number of carbon atoms per molecule for both unreactive and reactive classes of hydrocarbons (NC_U and NC_R respectively) using

$$NC_U = \frac{\sum_i C_i (NC_U)_i}{\sum_i C_i}$$

TABLE 5. MONITORING LOCATIONS AT WHICH PLOTS OF CARBON MONOXIDE PREDICTIONS AND MEASUREMENTS WERE PREPARED FOR THE SIX VALIDATION DAYS

Station \ Day	29 Sept.	30 Sept.	29 Oct.	30 Oct.	4 Nov.	11 Sept.
Reseda	X	X	X	X	X	X
Burbank	X	X	X	X	X	X
Pasadena					X	
Azusa	X	X	X	X	X	X
El Monte	X	X		X	X	
Downtown LA	X	X	X	X	X	X
Pomona	X	X	X	X	X	X
West LA*	X	X	X	X	X	X
Commerce	X	X	X	X	X	X
Lennox*	X	X	X	X	X	X
Whittier*	X	X	X	X	X	X
La Habra						
Long Beach*	X	X	X	X	X	X
Anaheim			X	X	X	X
Santa Ana						

* Local corrections made for this station.

TABLE 6. MONITORING LOCATIONS AT WHICH PLOTS OF NITRIC OXIDE, NITROGEN DIOXIDE, AND OZONE PREDICTIONS AND MEASUREMENTS WERE PREPARED FOR THE SIX VALIDATION DAYS*

Station \ Day	29 Sept.	30 Sept.	29 Oct.	30 Oct.	4 Nov.	11 Sept.
Reseda	X	X	X	X	X	X
Burbank	X	X	X	X	X	X
Pasadena	X	X	X	X	X	X
Azusa	X	X	X	X	X	X
El Monte	X	X	only NO_2 and O_3	only O_3	X	only O_3
Downtown LA	X	X	X	X	X	X
Pomona	X	X	X	X	X	X
West LA	X	X	X	X	X	X
Commerce	X	X	X	X	X	only NO and O_3
Lennox	X	X	X	X	X	X
Whittier	X	X	X	X	X	X
La Habra	X	X	only NO_2	only NO and NO_2	X	X
Long Beach	X	X	X	X	X	X
Anaheim	X	X	X	X	X	X
Santa Ana	← only ozone →					

*Mark (X) indicates all three pollutants measured at station for the particular day. For each station, nitric oxide and nitrogen dioxide are plotted on a single figure, while ozone is plotted on a second figure. Each set of two figures are presented on one page.

TABLE 7. MONITORING LOCATIONS AT WHICH PLOTS OF TOTAL HYDROCARBON PREDICTIONS AND MEASUREMENTS WERE PREPARED FOR THE SIX VALIDATION DAYS

Station \ Day	29 Sept.	30 Sept.	29 Oct.	30 Oct.	4 Nov.	11 Sept.
Pasadena	X	X	X	X	X	X
Azusa	X	X	X	X	X	X
El Monte	X	X			X	
Downtown LA	X	X	X	X	X	X
Commerce	X	X			X	
Anaheim	X	X			X	

FIGURE 14.

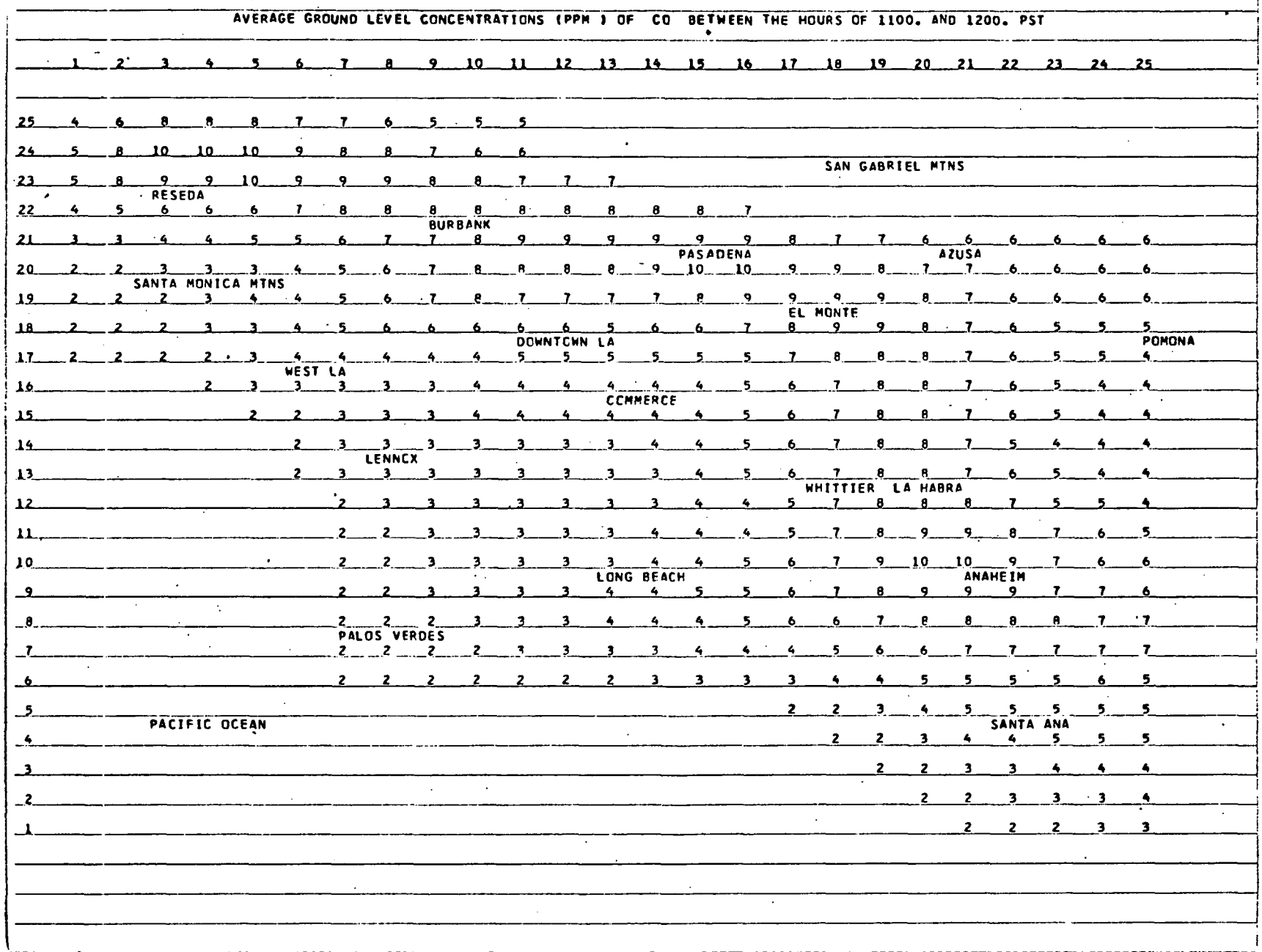
AVERAGE GROUND LEVEL CONCENTRATIONS (PPM) OF CO BETWEEN THE HOURS OF 1100. AND 1200. PST
1 2 3 4 5 6 7 8 9 10 11 12 13 14 15 16 17 18 19 20 21 22 23 24 25
25 4 6 8 8 8 7 7 6 5 5 5
24 5 8 10 10 10 9 8 8 7 6 6
23 5 8 9 9 10 9 9 9 8 8 7 7 7
SAN GABRIEL MTNS
RESEDA
22 4 5 6 6 6 7 8 8 8 8 8 8 8 8 8 8 7
BURBANK
21 3 3 4 4 5 5 6 7 7 8 9 9 9 9 9 9 8 7 7 6 6 6 6 6 6
PASADENA
AZUSA
20 2 2 3 3 3 4 5 6 7 8 8 8 8 9 10 10 9 9 8 7 7 6 6 6 6
SANTA MONICA MTNS
19 2 2 2 3 4 4 5 6 7 8 7 7 7 7 8 9 9 9 9 8 7 6 6 6 6
EL MONTE
18 2 2 2 3 3 4 5 6 6 6 6 6 5 6 6 7 8 9 9 8 7 6 5 5 5
DOWNTOWN LA
POMONA
17 2 2 2 2 3 4 4 4 4 4 5 5 5 5 5 5 7 8 8 8 7 6 5 5 4
WEST LA
16 2 3 3 3 3 3 4 4 4 4 4 4 5 6 7 8 8 7 6 5 4 4
COMMERCE
15 2 2 3 3 3 4 4 4 4 4 4 5 6 7 8 8 7 6 5 4 4
14 2 3 3 3 3 3 3 3 4 4 5 6 7 8 8 7 5 4 4 4
LENNOX
13 2 3 3 3 3 3 3 3 3 4 5 6 7 8 8 7 6 5 4 4
WHITTIER LA HABRA
12 2 3 3 3 3 3 3 3 4 4 5 7 8 8 8 7 5 5 4
11 2 2 3 3 3 3 3 4 4 4 5 7 8 9 9 8 7 6 5
10 2 2 3 3 3 3 3 4 4 5 6 7 9 10 10 9 7 6 6
LONG BEACH
ANAHEIM
9 2 2 3 3 3 3 4 4 5 5 6 7 8 9 9 9 7 7 6
8 2 2 2 3 3 3 4 4 4 5 6 6 7 8 8 8 8 7 7
PALOS VERDES
7 2 2 2 2 3 3 3 3 4 4 4 5 6 6 7 7 7 7 7
6 2 2 2 2 2 2 2 3 3 3 3 4 4 5 5 5 5 6 5
5 2 2 3 4 5 5 5 5 5
PACIFIC OCEAN
SANTA ANA
4 2 2 3 4 4 5 5 5
3 2 2 3 3 4 4 4
2 2 2 3 3 3 4
1 2 2 2 3 3

FIGURE 15.

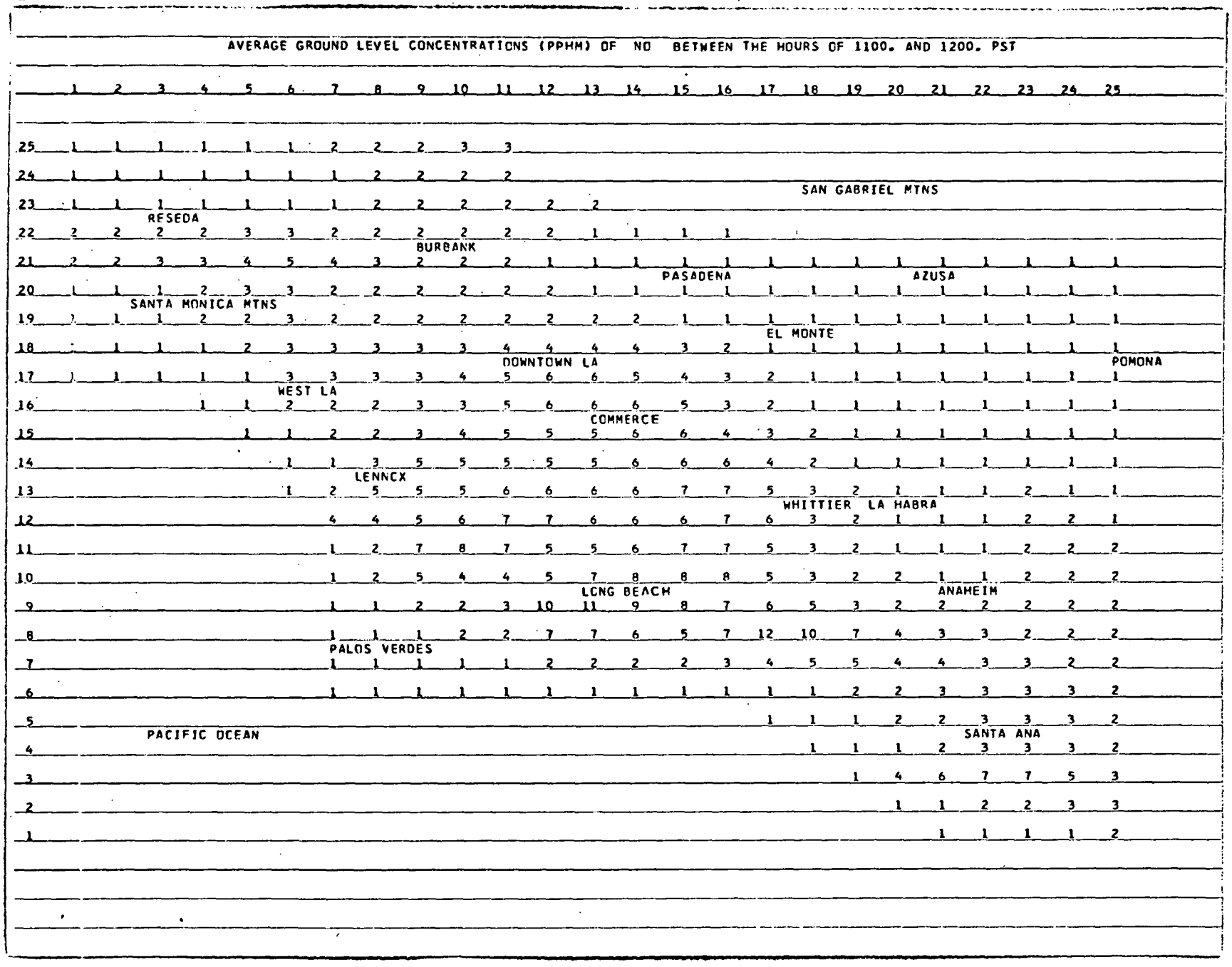
AVERAGE GROUND LEVEL CONCENTRATIONS (PPHM) OF NO BETWEEN THE HOURS OF 1100. AND 1200. PST
1 2 3 4 5 6 7 8 9 10 11 12 13 14 15 16 17 18 19 20 21 22 23 24 25
25 1 1 1 1 1 1 2 2 2 3 3
24 1 1 1 1 1 1 1 2 2 2 2
23 1 1 1 1 1 1 1 1 2 2 2 2 2 2
22 2 2 2 2 3 3 2 2 2 2 2 2 1 1 1 1
21 2 2 3 3 4 5 4 3 2 2 2 1 1 1 1 1 1 1 1 1 1 1 1 1 1
20 1 1 1 2 3 3 2 2 2 2 2 2 1 1 1 1 1 1 1 1 1 1 1 1 1
19 1 1 2 2 3 2 2 2 2 2 2 2 2 1 1 1 1 1 1 1 1 1 1 1 1
18 1 1 1 2 3 3 3 3 3 4 4 4 4 3 2 1 1 1 1 1 1 1 1 1 1
17 1 1 1 1 1 3 3 3 4 5 6 6 5 4 3 2 1 1 1 1 1 1 1 1 1
16 1 1 2 2 2 3 3 5 6 6 6 5 3 2 1 1 1 1 1 1 1 1 1
15 1 1 2 2 3 4 5 5 5 6 6 4 3 2 1 1 1 1 1 1 1 1
14 1 1 3 5 5 5 5 5 6 6 6 4 2 1 1 1 1 1 1 1 1
13 1 2 5 5 5 6 6 6 6 7 7 5 3 2 1 1 1 2 1 1
12 4 4 5 6 7 7 6 6 6 7 6 3 2 1 1 1 2 2 1
11 1 2 7 8 7 5 5 6 7 7 5 3 2 1 1 1 2 2 2
10 1 2 5 4 4 5 7 8 8 8 5 3 2 2 1 1 2 2 2
9 1 1 2 2 3 10 11 9 8 7 6 5 3 2 2 2 2 2 2
8 1 1 1 2 2 7 7 6 5 7 12 10 7 4 3 3 2 2 2
7 1 1 1 1 1 2 2 2 2 3 4 5 5 4 4 3 3 2 2
6 1 1 1 1 1 1 1 1 1 1 1 1 2 2 3 3 3 3 2
5 1 1 1 2 2 3 3 3 2
4 1 1 1 2 3 3 3 2
3 1 4 6 7 7 5 3
2 1 1 2 2 3 3
1 1 1 1 1 2
SAN GABRIEL MTNS
RESEDA
BURBANK
PASADENA
AZUSA
SANTA MONICA MTNS
EL MONTE
DOWNTOWN LA
POMONA
WEST LA
COMMERCE
LENNOX
WHITTIER
LA HABRA
LONG BEACH
ANAHEIM
PALOS VERDES
PACIFIC OCEAN
SANTA ANA

FIGURE 16.

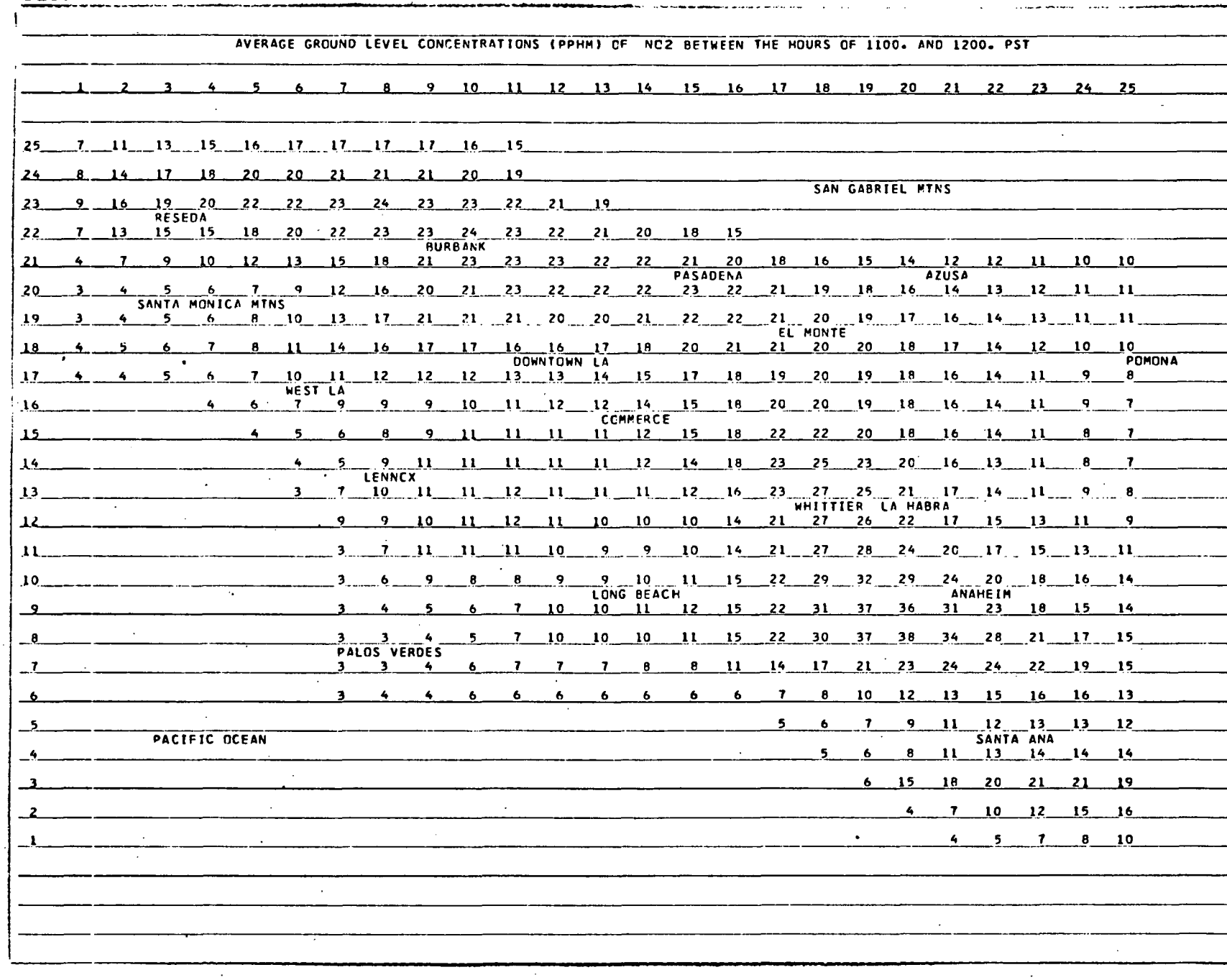
AVERAGE GROUND LEVEL CONCENTRATIONS (PPHM) OF NO2 BETWEEN THE HOURS OF 1100. AND 1200. PST
1 2 3 4 5 6 7 8 9 10 11 12 13 14 15 16 17 18 19 20 21 22 23 24 25
25 7 11 13 15 16 17 17 17 17 16 15
24 8 14 17 18 20 20 21 21 21 20 19
23 9 16 19 20 22 22 23 24 23 23 22 21 19
SAN GABRIEL MTNS
RESEDA
22 7 13 15 15 18 20 22 23 23 24 23 22 21 20 18 15
BURBANK
21 4 7 9 10 12 13 15 18 21 23 23 23 22 22 21 20 18 16 15 14 12 12 11 10 10
PASADENA
AZUSA
20 3 4 5 6 7 9 12 16 20 21 23 22 22 22 23 22 21 19 18 16 14 13 12 11 11
SANTA MONICA MTNS
19 3 4 5 6 8 10 13 17 21 21 21 20 20 21 22 22 21 20 19 17 16 14 13 11 11
EL MONTE
18 4 5 6 7 8 11 14 16 17 17 16 16 17 18 20 21 21 20 20 18 17 14 12 10 10
DOWNTOWN LA
POMONA
17 4 4 5 6 7 10 11 12 12 12 13 13 14 15 17 18 19 20 19 18 16 14 11 9 8
WEST LA
16 4 6 7 9 9 9 10 11 12 12 14 15 18 20 20 19 18 16 14 11 9 7
COMMERCE
15 4 5 6 8 9 11 11 11 11 12 15 18 22 22 20 18 16 14 11 8 7
14 4 5 9 11 11 11 11 11 12 14 18 23 25 23 20 16 13 11 8 7
LENNOX
13 3 7 10 11 11 12 11 11 11 12 16 23 27 25 21 17 14 11 9 8
WHITTIER
LA HABRA
12 9 9 10 11 12 11 10 10 10 14 21 27 26 22 17 15 13 11 9
11 3 7 11 11 11 10 9 9 10 14 21 27 28 24 20 17 15 13 11
10 3 6 9 8 8 9 9 10 11 15 22 29 32 29 24 20 18 16 14
LONG BEACH
ANAHEIM
9 3 4 5 6 7 10 10 11 12 15 22 31 37 36 31 23 18 15 14
8 3 3 4 5 7 10 10 10 11 15 22 30 37 38 34 28 21 17 15
PALOS VERDES
7 3 3 4 6 7 7 7 8 8 11 14 17 21 23 24 24 22 19 15
6 3 4 4 6 6 6 6 6 6 6 7 8 10 12 13 15 16 16 13
5 5 6 7 9 11 12 13 13 12
PACIFIC OCEAN
SANTA ANA
4 5 6 8 11 13 14 14 14
3 6 15 18 20 21 21 19
2 4 7 10 12 15 16
1 4 5 7 8 10